universität wien

MASTERARBEIT / MASTER‘S THESIS

Titel der Masterarbeit / Title of the Master’s Thesis

“Radiosyntheses of PET-Tracers for Platelets-Labelling”

verfasst von / submitted by

Sophie Pichler BSc

angestrebter akademischer Grad / in partial fulfilment of the requirements for the degree of

Master of Science (MSc)

Wien, 2023 / Vienna 2023

Studienkennzahl lt. Studienblatt / degree programme code as it appears on the student record sheet:	A 066 862
Studienrichtung lt. Studienblatt / degree programme as it appears on the student record sheet:	Masterstudium Chemie
Betreut von / Supervisor:	Assoz. Prof. Mag. Dr. Wolfgang Wadsak, Privatdoz.

Acknowledgments

Working on a Master's thesis can be challenging at times. Therefore, I would like to express my gratitude to all the people who supported me along the way.

Firstly, I would like to thank Assoc. Prof. Dr. Wolfgang Wadsak for the opportunity to carry out my Master's thesis under his supervision.

Special thanks go to Dr. Chrysoula Vraka for her constant support, guidance and encouragement during the practical as well as the written part. Also, thank you for the thought-provoking conversations and the numerous blood donations.

I would also like to express my gratitude to all the members of the various research groups, as well as the radio technicians for the many blood donations and their helpful comments. Special thanks to Fritz for all the blood withdrawals, for all the wonderful pieces of advice and for all the funny conversations while enjoying lots of Toffifee. Thanks to the committed blood donors Eva, Viktoria, Stefan, Nati, Anna, Paulina and everyone else. I really appreciated that!

Special thanks to my parents and my siblings for your constant emotional support, patience and motivation. Without you, I would not have been able to complete my studies. Thanks for always having my back!

Last, but not least, I would like to thank my friends for the incredibly lovely moments, the support and the mutual encouragement. Many thanks to Miriam, Alexander, Theresa, Hannah, Dorith and Dani. A special thank you goes to you, Lisza, for all the advice and your incredible patience with me.
Thank you very much!

Abstract

Platelets participate in many different biological processes, including various pathogenesis as in cardiovascular diseases. Their multifunctional character makes them desirable labelling targets for diagnostic imaging.

The SPECT tracer [^{111}In]In-oxine is currently the gold standard for labelling isolated, non-activated platelets. However, developments in various areas of medicine, such as immunology or cell-based therapy, are creating new challenges for diagnostic imaging which are not met by SPECT. Due to the possibility of quantification, the higher spatial resolution, as well as the better sensitivity compared to SPECT applications, PET imaging can be used to fulfil the requirements of detecting small lesions, for example. However compared to [^{111}In]In-oxine, only lower labelling values have been achieved using the PET tracer [^{68}Ga]Ga-oxine in platelets. Accordingly, the aim of this thesis was to optimise the synthesis protocol as well as the isolation and labelling procedures in order to achieve higher labelling efficiencies, similar to those of [^{111}In]In-oxine.

Besides the successful production of [^{68}Ga]Ga-oxine, the long-lived PET tracer [^{89}Zr]Zr-oxine was also synthesised with high radiochemical conversation rates. The experiments with [^{111}In]In-oxine served as basis to understand the beneficial conditions to subsequently integrate them into platelet labelling with PET tracers. Despite modifications of the isolation process, no higher labelling efficiencies than 25% were achieved using [^{68}Ga]Ga-oxine. However, the isolated, non-activated platelets were labelled with sufficiently high efficiency (39% LE) for the first time with [^{89}Zr]Zr-oxine.

A central aspect for further investigations is the stability of both PET tracers under physiological conditions. Furthermore, the viability of the labelled platelets should be examined. Cell disruption methods will provide information on the binding site of the tracer (cell incorporation).

Zusammenfassung

Thrombozyten nehmen als Blutbestandteile an vielen verschiedenen biologischen Prozessen, darunter auch an diversen Entstehungsprozessen von Krankheiten, z.B. sind die relevant bei der Entstehung von kardiovaskulären Ereignissen, teil. Durch ihren multifunktionalen Charakter sind sie geeignete Markierungsziele für die diagnostische Bildgebung. Der SPECT-Tracer [^{111}In]In-oxine ist der momentane Goldstandard für die Markierung von isolierten, nicht-aktivierten Thrombozyten. Durch die Entwicklungen in diversen medizinischen Disziplinen, wie in der Immunologie oder Onkologie z.B. durch zellbasierte Therapien, werden neue Ansprüche, die von der SPECT-Methode nicht erfüllt werden, an die diagnostische Bildgebung gestellt. Aufgrund der Möglichkeiten der Quantifizierung, der höheren räumlichen Auflösung, sowie der besseren Sensitivität im Vergleich zu SPECT-Anwendungen, können über PET-Bildgebungen die Anforderungen, die beispielsweise eine Detektion kleiner Läsionen stellt, erreicht werden. Im Unterschied zu [^{111}In]In-oxine konnten mit dem PET-Tracer [^{68}Ga]Ga-oxine allerdings nur niedrigere Markierungswerte bei Thrombozyten erreicht werden.

Demnach war das Ziel dieser Masterarbeit die Optimierung der Synthesevorschriften, wie auch der Isolierungs- und Markierungsprotokolle, um höhere, mit [^{111}In]In-oxine vergleichbare, Zellaufnahmen zu erreichen.

Neben der erfolgreichen Herstellung von [^{68}Ga]Ga-oxine, konnte auch der langlebige PET-Tracer [^{89}Zr]Zr-oxine mit hohen radiochemischen Umsatzraten synthetisiert werden. In Experimenten mit [^{111}In]In-oxine konnten vorteilhafte Bedingungen herausgefunden werden und entsprechend für die Thrombozyten-Markierungen mit den PET-Tracern verwertet werden. Trotz diverser Modifikationen des Isolierungsverfahrens wurden mit [^{68}Ga]Ga-oxine keine höheren Markierungseffizienzen als 25% erreicht. Jedoch konnten zum ersten Mal isolierte, nicht aktivierte Blutplättchen mit ausreichend hoher Effizienz (39%) mit [^{89}Zr]Zr-oxine markiert werden.

Für eine *in vivo* Anwendung, wird ein zentraler Punkt für weitere Untersuchungen die Stabilität beider PET-Radiotracer unter physiologischen Bedingungen. Außerdem sollte die Viabilität der markierten Thrombozyten im Detail überprüft werden. Zellaufschlussmethoden könnten die Frage nach einer Zell-Inkorporation des Tracers beantworten.

Table of Content

1. Introduction

1.1. Platelets

Platelets are involved in many, diverse biological processes, including a wide variety of pathogenesis as cardiovascular diseases. The multifunctional and dynamic nature of the cells makes them suitable targets for radiolabelling applications.[1] With a size of 3.6 x 0.7 µm, they represent the smallest components of blood.[2] Their lifespan is limited to 8–10 days, requiring continuous production to ensure a steady total platelet count, which averages between 150.000–400.000 cells/µl in a healthy person's body.[3] Platelet production is carried out by the precursor cells megakaryocytes in the bone marrow. All in all, 10^{11} cells are secreted per day.[4] Inside the anucleate and discoid-shaped platelets are various secretory granules, such as **α**-granules or lysosomes, which are enclosed by a phospholipid bilayer membrane with various adherent proteins, such as glycoproteins.[5] Most platelets remain in their resting, inactivated form in the blood flow during their lifetime only when tissue is damaged and bleeding occur, they become activated.[1] In detail, when damage is recognised, the circulating platelets respond rapidly by decelerating to adhere to the damaged subendothelial area *via* various interactions, releasing their intracellular granules to activate other circulating platelets as supports, thus forming an aggregate around the injured site to prevent bleeding.[3] In primary hemostasis (adhesion), van Willebrand factors (vWF) or collagen bind to various glycoprotein (GP) receptors on the cell membrane[4]. This interaction causes the release of secretory compounds, such as serotonin or Adenosin-Di-Phosphate (ADP), resulting in the assembly of more platelets, and a change in shape through development of pseudopodia.[2] As a result, glycoprotein IIB/IIIA receptors on the platelet membrane are activated, allowing fibrinogen to bind, in turn resulting in cross-linking of platelets that ultimately leads to aggregation.[6] The stability of the complex is increased during secondary hemostasis through the increased recruitment of platelets and the formation of thrombin and fibrin, followed by a stable '*red thrombus*'.[1]

1.1.1. Glycoprotein IIb/IIIa receptor

Due to its central function in the formation of aggregation, the GPIIb/IIIa receptor is a potential target for molecular imaging of thromboembolic diseases, such as myocardial infarction, transient ischemic attack, stroke, or pulmonary embolism.[7] However, labelling the receptor of activated platelets has not been very successful due to various factors, such as low

receptor affinity, slow secretion, low target-background ratio, or poor spatial resolution.[8] Anyway, good promising preclinical results have been reported from two novel radiotracers, a specific small molecule [^{18}F]F-GP1[7] and a specific single-chain antibody [^{64}Cu]CuMeCOSar[9]. [^{18}F]F-GP1 is an analogue of elarofiban produced *via* nucleophilic radio fluorination of the precursor and shows some beneficial properties, such as high specificity to the GPIIb/IIIa receptor, rapid elimination and a high signal-to-noise ratio.[7, 8] Promising results in acute venous thromboembolism (VTE) imaging suggest that [^{18}F]F-GP1 may overcome some limitations of previous tracers, such as a possible distinction between acute and chronic VTE.[10] A GMP-compliant synthesis of [^{18}F]F-GP1 has been presented by Hugenberg *et al*.[11] In addition, a successful application of the [^{18}F]F-GP1 tracer in thrombus formation on bioprosthetic aortic valves in patients has recently been reported by Bing *et al.*[12]

However, platelet functions are not limited to hemostasis and coagulation. They are involved in many pathophysiological processes, such as inflammation, atherogenesis, tumourigenesis or metastasis, diabetes mellitus, or Alzheimer's disease, which make them a promising marker.[1, 13]

1.2. Labelling of Platelets

Non-activated platelets were first labelled with the radioisotope chromium-51 before indium-111 was introduced by Thakur *et al*. Through platelet labelling, increased knowledge was gained on their physiology and on various pathophysiological processes.[14] Platelet labelling has been applied for imaging of deep vein thrombosis (DVT)[15, 16, 17], intracardiac thrombi[18], pulmonary embolism[19], atherosclerosis[14], hematologic diseases (e.g. idiopathic thrombocytopenic purpura[20]), acute vascular rejection due to platelet deposition after transplantation[21], or platelet recovery and survival after transfusion[22].

Indium-111 oxine (*vide infra*) has emerged as the gold standard for platelet labelling, whereby platelets are incubated *ex vivo* with the radiotracer, and then reinjected into the imaging subject to follow the distribution of the labelled cells *in vivo*. [^{111}In]In-oxine is best described as a radio-ionophore complex for direct cell labelling. Due to the lipophilic character of the ligand 8-hydroxyquinoline (oxine, ionophore) diffusion through the cell membrane of the $^{111}In^{3+}$-ion is enabled. As a result of the non-specific affinity, the cell population to be labelled must be as homogeneous as possible to avoid false interpretations.[19]

In addition, the viability and function of the cells should not be altered by the radiotracer, the isolation, or the labelling process. When labelling platelets, adverse conditions to the

biological matrix should be kept to a minimum to prevent platelet activation. However, labelling in plasma is usually not advisable due to the high binding affinity of radiotracers to plasma proteins (*vide infra*). Therefore, the best possible conditions must be selected depending on the cells, the radiotracer, and the demands.[23, 24]

1.3. Indium

In aqueous solutions indium is mainly present in the oxidation state +III. According to Pearson's hard and soft acid-base theory (HSAB), In^{3+} is a relatively hard acid, and therefore reacts with hard bases, preferably with oxygen or nitrogen ligands.[25]

1.3.1. Indium-111

With two gamma emissions (171.3 and 254.4 kEV) and a half-life of 2.83 days, the radioisotope indium-111 is well suited for long-term single photon emission computed tomography (SPECT) imaging and can therefore serve as a radiotracer for monoclonal antibodies or cellular blood components.[26] The most common way to produce the radioisotope is by cyclotron *via* the reaction $^{112}Cd(p, 2n)^{111}In$.[27]

1.3.1.1. Indium-111 oxine

Over many years, the well-established [^{111}In]In-oxine tracer has been used to label a wide variety of cell types, such as white blood cells (WBCs) and red blood cells (RBCs)[28], platelets[29], **γδ**-T cells[30] or mesenchymal stem cells[19, 31],. In addition, similar ligand systems, such as tropolone[32, 33] or 2-mercapto-pyridin-N-oxide (MPO)[34], have been reported for the corresponding labelling with indium-111.[24] However, oxine binds to the In^{3+}-ion in a 3:1 ratio, forming a neutral complex [^{111}In][In(oxinate)$_3$] that acts as an ionophore (see figure 1).[35] The mechanism of indium-111 oxine is best described as a passive diffusion through the lipid bilayer cell membrane enabled by the lipophilic ligands. Due to the relatively low binding affinity between In^{3+} and oxine, dissociation occurs within the cell, whereby In^{3+} becomes trapped by binding to cell compartments while the free ligand oxine is released from the cell.[19, 36, 37]

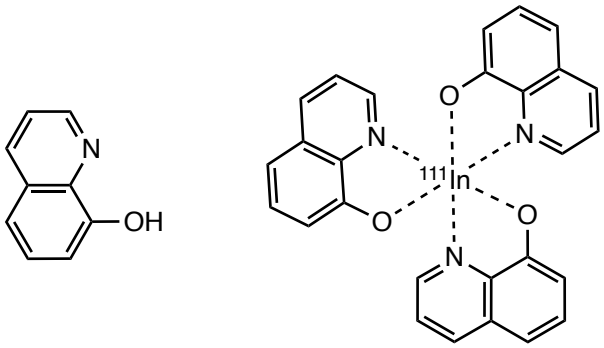

Figure 1: Structure of the ligand 8-hydroxyquinoline (oxine, left) and of the complex [^{111}In][In(oxinate)$_3$] (right).

1.4. 8-Hydroxyquinoline (Oxine)

8-hydroxyquinoline is a heterocyclic bidentate ligand that coordinates *via* the pyridyl nitrogen and the hydroxy group to a variety of metal atoms, including In^{3+}, Ga^{3+} and Zr^{3+}, forming a neutral complex through the deprotonation of the hydroxy group (see figure 1).[19] The ligand oxine and corresponding derivatives of oxine have gained interest as drug candidates with regard to possible anti-cancer, anti-fungal as well as anti-microbial properties. [35, 38]

1.5. SPECT *vs*. PET

With the improvements in cell-based therapies, the current gold standard for cell labelling, [^{111}In]In-oxine, measured *via* SPECT, cannot meet all new requirements. For the detection of small lesions or of low cell numbers, the need for a suitable positron emission tomography (PET) tracer, providing more precise imaging, has grown.[39] In addition, the better spatial resolution and sensitivity of PET compared to SPECT allows the use of lower activity of the radiotracers.[40] Furthermore, PET enables quantitative analyses.[41] Whole-body PET applications will further improve sensitivity as well as spatial resolution, which in turn will also lead to a reduced amount of radiotracer required.[42]

The β^+-emitter gallium-68, for example, is a suitable PET isotope for cell labelling. However, longer biological processes cannot be analysed with gallium-68 due to its relatively short half-life of 68 min. Therefore, β^+-emitters with longer half-lives are preferable, such as zirconium-89 with a half-life of 78,4 h.[40]

1.6. Gallium

Essentially, there are three isotopes of gallium, ^{66}Ga, ^{67}Ga and ^{68}Ga, that are relevant for radiochemistry. Gallium-67 is a cyclotron-produced radioisotope with a half-life of 78.3 h and

suitable characteristics for a long-term SPECT radiotracer[43], while the cyclotron-produced β^+-emitter (56.5%) gallium-66 with a half-life of 9.49 h, is appropriate for long term PET imaging.[44] In addition, Gallium-68, also a β^+-emitter (90%, 1.83 MeV) with a relatively short half-life of 68 min is suitable for PET-analysis.[45]

In almost all radiopharmaceutical reactions, gallium is present in the oxidation state +III.[46] The Ga^{3+}-ion, like the In^{3+}-ion, is a hard Lewis acid which prefers to form complexes with hard Lewis bases, such as oxygen or nitrogen.[25, 47] At the maximum coordination number of six, *pseudo*-octahedral complexes are generally found.[48] Due to the similar ionic radius and a similar electronegativity as the high-spin Fe^{3+}-ion, the complex chemistry of gallium(III) as well as the chemical behaviour, in general, is similar to iron.[49, 50] However, the redox behaviour of the two differs significantly, as Ga^{3+}-ions do not undergo redox reactions under physiological conditions[50]. Given the similarity of the two ions, Ga^{3+} can also interact with various Fe^{3+} binding sites of diverse biological systems, such as those of the iron transporter transferrin.[51] Since the Ga^{3+}-transferrin-complex has a relatively high binding constant (logK = 20.3), a gallium complex used in plasma must have a higher stability or a kinetic inertness to prevent the interaction with transferrin.[52] An alternative to avoid complexation with transferrin during cell labelling is a prior removal of all transferrin proteins, which requires additional steps in the cell isolation process.[19]

In a pH range of 3–7 in an aqueous environment, gallium(III) forms various monomeric as well as polycationic hydroxide forms, with the low-soluble $Ga(OH)_3$ presenting the major difficulty for possible further reactions.[53, 54] Above pH > 7, gallium(III) is present as an unreactive $[Ga(OH)_4]^-$ and is therefore no longer accessible for reactions.[54] By adding stabilizing, weak ligands, such as EDTA, citrate or acetate, the hydroxide formation can be prevented by the formation of an intermediate complex, which in turn can react further in the presence of stronger-binding ligands.[45, 52, 54]

1.6.1. Gallium-68

The radioisotope gallium-68 with a half-life of 68 min is suitable for low-molecular peptides, antibody fragments, siderophores as well as for cell labelling.[55, 56] Due to the production *via* a mother/daughter-generator, gallium-68 is easily available and cheap in production[55]. As a result of increased demand in recent years, the production of gallium-68 by a cyclotron with zinc-68 as a solid target ($^{68}Zn(p,n)^{68}Ga$) is gaining importance.[57] However, gallium-68 is mainly produced *via* a $^{68}Ge/^{68}Ga$ generator. Germanium-68, with a half-life of 271 d, decays to

gallium-68 *via* electron capture. The decay product of gallium-68 *via* a β^+-emission (88%) is the zinc-68 isotope.[54, 58] Based on the great differences in the half-lives, a secular equilibrium exists between $^{68}Ge/^{68}Ga$[59], which enables the use of the generators for 1–2 years.[47] There are different types of generators, whereby for example, Ge-68 can be embedded in an organic or inorganic matrix, such as TiO_2, SnO_2 or ZrO_2, of a chromatographic column.[60, 61] As a result of the different chemistry of germanium and gallium, the short-lived gallium-68 can be effectively separated from germanium-68 *via* elution with aqueous HCl and obtained as $^{68}GaCl_3$.[47] Afterwards, the gallium-68 solution has to be analysed for a possible germanium-68 breakthrough,[57] The different types of generators have various advantages as well as disadvantages, such as metal impurities of the eluate are higher using an inorganic matrix instead of an organic one. Fractionation, post-purification, or post-processing can eliminate various disadvantages, such as excessive eluate volume or impurities.[58]

1.6.1.1. Gallium-68 oxine

As a PET alternative to the well-established SPECT tracer [^{111}In]In-oxine, [^{68}Ga]Ga-oxine was first introduced by Welch *et al.* (see figure 2).[62] As both elements belong to the 13th group in the periodic table, they behave in some ways similar, but they also differ: for example, the In^{3+}-ion is much larger than the Ga^{3+}-ion leading to different ligand affinities.[25] Accordingly, Ga^{3+} binds the ligand 8-hydroxquinoline (oxine) more strongly than In^{3+}.[63] Therefore, gallium-68 oxine can be used for labelling RBCs, platelets[62, 63] or CAR T cells.[56] In addition, [^{68}Ga]Ga-oxine labelled RBCs have been applied for in-human PET/CT analyses.[64, 65, 66] The cold compound gallium-oxine, KP46, is currently being investigated as an anticancer drug candidate for solid tumours, such as melanoma[67], osteosarcoma[68] as well as renal carcinoma, whereby the exact mechanism of KP46 has not been fully understood yet[69] and reported to show high stability under physiological conditions[70, 71].

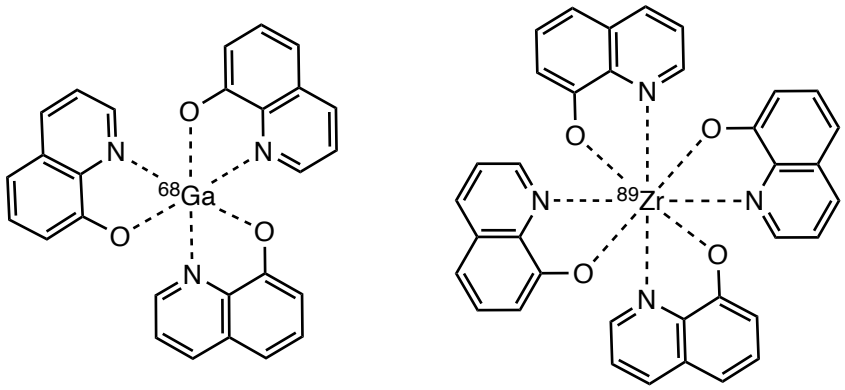

Figure 2: Structures of the complex [^{68}Ga][Ga(oxinate)$_3$] (left) and of the complex [^{89}Zr][Zr(oxinate)$_4$] (right).

1.7. Zirconium

Due to the similar complex chemistry and similar reactivity patterns as the SPECT isotope indium-111, the β^+-emitter zirconium-89 with a half-life of 78.4 h, which is for examples suitable for the imaging of antibodies (immuno-PET) can be used as a PET analogue.[19, 72] The element zirconium is located within the titanium group, the fourth transition group, with a high charge within a relatively small ionic radius. Due to the high charge density, it is an electropositive element with a resulting high reduction potential.[73] The transition metal occurs preferably in oxidation state +IV alongside +I, +II, +III.[74] However, Zr-ions with a charge below 4+ are not stable in aqueous systems, as they reduce H_2O to H_2 and/or disproportionate.[73, 74] In aqueous solutions, Zr^{4+}-ions form mono- or polynuclear hydroxo-complexes.[75] According to the HSAB theory, Zr^{4+} coordinates as a hard acid with up to eight coordination sites in the first sphere, preferably with oxygen and nitrogen atoms.[73, 76]

1.7.1. Zirconium-89

In radiochemistry, ^{89}Zr is mainly used, which decays to 23% *via* β^+-emission and to 77% *via* electron capture to the very short-lived ^{89m}Y (half-life $t_{1/2}$ = 15.7 s), which in turn decays to the stable ^{89}Y *via* γ-emission.[72, 45] There are two reactions, ^{89}Y(p,n)^{89}Zr and ^{89}Y(d,2n)^{89}Zr, for the production of zirconium-89.[77] However, the radioisotope is mainly cyclotron-produced *via* the first reaction by the bombardment of a solid yttrium foil.[73] A proton bombardment of an ^{89}Y target can basically give three reactions, ^{89}Y(p,n)^{89}Zr, ^{89}Y(p,pn)^{88}Y and ^{89}Y(p,2n)^{88}Zr[73]. By precisely adjusting the irradiation time and energy of the proton beam, the impurities in the form of the long-lived nuclides can be kept as low as possible.[78] The yttrium foil is then dissolved with a 1–6 M HCl and diluted with H_2O to keep the resulting HCl content below < 2 M for subsequent separation steps.[45, 73] Impurities generated during production, such as ^{56}Co, ^{48}V and ^{156}Tb, originating from the yttrium foil, as well as the long-lived nuclides ^{88}Zr and ^{88}Y,

are removed by solid-phase extraction (SPE) packed with hydroxamate resin.[73] Subsequently, washing is carried out with aqueous HCl and high-purity H_2O before the $^{89}Zr^{4+}$-ions are eluted by 1 M oxalic acid as [^{89}Zr]Zr-oxalate, resulting in 99.99% radiochemical purity (RCP).[45]

Given the half-life of zirconium-89, the radioisotope is mainly used in antibody-based PET imaging (immuno-PET).[79] From a chemical point of view, a polydentate ligand with a coordination number of preferably eight and a high, negative charge to counteract the Zr^{4+}-ion to form a stable complex is an ideal binding partner.[76] The six-dentate ligand desferrioxamine (DFO), which binds to the radiometal zirconium-89 through three hydroxamates, was the first chelator for Zr-89 to be used in human experiments.[45] Based on reported non-specific uptake in bones of ^{89}Zr-DFO in mice, instability of the complex *in vivo* is assumed.[80] Accordingly, intensive research has been carried out in recent years on possible, more stable alternatives to DFO that suit the eight coordination sites of Zr-89 and thus provide enhanced stability.[79]

In addition to its long half-life, zirconium-89 is beneficial for biological processes as biological surrogacy of ferric ions.[81] The focus of zirconium radiochemistry is on antibody labelling, yet there are several other applications, such as protein or cell labelling.[79] Although the gold standard for cell labelling indium-111 prefers the oxidation state +III, certain similarities in reactivity and ligand chemistry between the two makes $^{89}Zr^{4+}$ a possible PET analogue.[19, 82] Various zirconium complexes in form of ZrL_4 have been synthesised with various bidentate ligands already used with indium-111, such as tropolone or oxine (see figure 2), for labelling, for example, extracellular vesicles[83], liposomes[84, 85] or different cell types such as CAR T-cells[86], toxic T-cells and dendritic cells[87], $\gamma\delta$-T-cells[88], leukocytes[39, 82] or RBCs[40].

2. Aim of Thesis

The aim of this thesis was the labelling of isolated, non-activated platelets for PET imaging using synthesised lipophilic PET tracers, e.g. [^{68}Ga]Ga-oxine and [^{89}Zr]Zr-oxine enabling cell labelling. Therefore, optimisation of both literature-known syntheses of the radiotracers, platelet isolation and labelling shall be performed.

Firstly, improved and reproducible results of [^{68}Ga]Ga-oxine and [^{89}Zr]Zr-oxine should be obtained by modifications of synthesis parameters. The produced complexes should be examined for their conversion rates and stabilities *via* iTLC measurements.

In the next step, experiments with the well-established SPECT tracer for platelet labelling [^{111}In]In-oxine should provide information about preferred incubation conditions and parameters and should subsequently be conducted in the labelling experiments using the PET tracers, [^{68}Ga]Ga-oxine and [^{89}Zr]Zr-oxine. The main object was to achieve sufficient, reproducible labelling efficiencies in platelets with the PET tracers and thus provide a basis for *in vivo* experiments.

3. Materials and Methods

3.1. Materials and Instrumentations

The chemicals used were purchased from commercial producers (B. Braun Melsungen AG, Citra Labs LLC, Curium Netherlands B.V., Gibco™, Greiner Bio-One, Honeywell, Merck KGaA, Morphisto GmbH, Perkin Elmer®, Rotem Industries Ltd. and Sigma Aldrich) and used without further processing. They are summarised in table 38 in the appendix.

Three different radiometals were used for the experiments. [^{68}Ga]$GaCl_3$ was eluted directly in 1.1 ml metal-free HCl from a TiO_2-based $^{68}Ge/^{68}Ga$ generator (Galli Ad 0.741.85 GBq, Radionuklidgenerator, IRE ELit) with activities of > 300 MBq. For the zirconium complexations, [^{89}Zr]Zr-oxalate (*NEZ308000MC*, Perkin Elmer®) was commercially purchased with an activity of > 400 MBq. For the labelling experiments with indium, the commercially available [^{111}In]In-oxinate (*DRN 4908*, Curium Netherlands B.V.) with an activity of > 37 MBq was obtained.

The complex formation and radiochemical conversion of the synthesised tracers were analysed *via instant* thin layer chromatography (iTLC). Instant-TLC-SG-Glass microfiber chromatography paper impregnated with silica gel (*SGI0001*, Agilent Technologies) and Whatman no.1. papers (Whatman®) were used. The chromatography plates were read using the radio TLC scanner Gina Star (for gallium-68 and indium-111; Raytest) as well as the miniGita Dual (for zirconium-89; Elysia Raytest) and evaluated using the GINA STAR TLC™ software (Version 6.3). $CHCl_3$/CH_3OH (95:5) or 100% EtOAC (for Whatman no.1. papers) were used as mobile phases.

The activities were measured with a 2480 WIZARD^2 3” Automatic Gamma Counter (*2480-0010*, Perkin Elmer®) as well as with a dose calibrator (AktivimeterISOMED 2010, MED Nuklear-Medizintechnik Dresden GmbH).

The centrifugation steps were carried out using two different centrifuges. For cell culture experiments, the Rotanta 460 RC (*5670*, Hettich GmbH & Co KG) was used. All other centrifugation steps were performed using the Universal 320 R (*1406*, Hettich GmbH Co & KG). *Via* the Luna™ Automated cell counter (*L10001*, Logos) the cell numbers were determined. All devices used are listed in table 40 in the appendix.

In general, common synthesis materials such as tubes, vials, pipettes etc. were used from commercial suppliers (ABX, Eppendorf Tubes®, Thermo Fischer Scientific etc.). Some specific materials are shown in table 39 in the appendix.

3.2. Methods

3.2.1. Radiotracer-Syntheses

In total, three different synthesis approached were used to obtain the radiotracers [^{68}Ga]Ga-oxine and [^{89}Zr]Zr-oxine. [^{68}Ga]Ga-oxine was produced according to Sinzinger *et al*. Furthermore, [^{68}Ga]Ga-oxine as well as [^{89}Zr]Zr-oxine were synthesised *via* two additional methods – an on-cartridge method by Socan *et al.* and a kit formulation by Man *et al*.

Coordinating Radiometals

For gallium complexation, radiolabelled [^{68}Ga]$GaCl_3$ was obtained by elution in 1.1 ml 0.1 M metal-free HCl from a TiO_2-based ^{68}Ge/^{68}Ga generator. Zirconium was obtained commercially in form of [^{89}Zr]Zr-oxalate in 1 M oxalic acid with an activity of > 400 MBq.

In this chapter, the general methods are first described before various modifications of the parameters of the methods are discussed.

3.2.1.1. Sinzinger-Method

The method of Sinzinger *et al.* was developed by his research group (Department of Biomedical Imaging and Image-guided Therapy at AKH Vienna) based on previous work[89, 90] as well as the work of Thompson *et al.*[91] This method was carried out for synthesising [^{68}Ga]Ga-oxine.

General Procedure

The precursor 8-hydroxyquinoline (oxine, c = 2 mg/ml) was first dissolved in ethanol resulting in a clear yellow solution. 600 µl [^{68}Ga]$GaCl_3$ varying in activity was mixed with 30 µl saturated sodium acetate solution before 90 µl oxine was added. The mixture was then shaken for 15 min at room temperature (r.t.). The activity was measured using a dose calibrator. The radiochemical conversion was investigated by iTLC and after extraction into an *n*-octanol phase as described by Socan *et al.* (see chapter 3.2.1.4).[39]

Variations

The general procedure described above was varied for different parameters: various activities (7.9–20.0 MBq) of the radiometal, a 1 M and a 2 M sodium acetate solution at constant volume ratio (0.05 vol.eq.) instead of the saturated solution and increased volume of sat.

NaOAc (30 µl, 100 µL (0.19 vol.eq.) and 300 µL (0.91 vol.eq.)). An overview of the modified parameters is shown in table 1.

Table 1: Various experiments of [^{68}Ga]Ga-oxine according to Sinzinger et al. with modified parameters.

Variant	n	$V_{(Ga\text{-}Eluate)}$ [µl]	$V_{(NaOAc)}$ [µl]	$c_{(NaOAc)}$ [mol*L^{-1}]	$V_{(oxine)}$ [µl]	pH
Sinzinger	12	600	30	sat.	90	4.5–5.0
Sinzinger*/1V	9	530	100	sat.	90	5.5–6.0
2V	3	330	300	sat.	90	7.5–8.0
1M	3	600	30	1	90	0–1.0
2M	3	600	30	2	90	1.0–1.5

3.2.1.2. Socan-Method

The on-cartridge method developed by Socan *et al.* was published in 2019 and describes the syntheses of [^{68}Ga]Ga-oxine as well as [^{89}Zr]Zr-oxine.[40] In the following, the method is referred to as Socan-method or cartridge-method.

General Procedure

Via an on-cartridge method of Socan *et al.* [^{68}Ga]Ga-oxine and [^{89}Zr]Zr-oxine were synthesised. The QMA cartridge was conditioned with 2 ml of Milli-Q water before being dried with 5 ml of air. The radiometals ([^{68}Ga]$GaCl_3$ in 5 ml metal-free HCl: 26–40 MBq, [^{89}Zr]Zr-oxalate neutralized with 1 M Na_2CO_3 (1:1): 2 MBq, filled up to 500 µl with ultrapure H_2O) were mixed with NaOAc (c = 155 mg/ml, for gallium: V = 1 ml, zirconium: V = 250–300 µl) and were applied on cartridge. After the cartridge was dried, the radioactivity retained on the cartridge and of the eluate was measured to calculate the loading efficiency (LoE). Then, 300 µl 8-hydroxyquinoline (c = 1 mg/ml), dissolved in Milli-Q H_2O with 20% EtOH for gallium-68 and with 50% EtOH for zirconium-89, was loaded on cartridge. To allow formation of the gallium complex, incubation was performed for 10 min before eluting with 2 ml PBS. For the zirconium complex, incubation was done twice with 300 µl oxine solution each for 60 min before the complex was washed from the cartridge. The pH value was measured, and the yield was determined by measuring the remaining activity on the cartridge and the activity of the eluate and illustrated as percent rate. The RCC was evaluated by iTLC and after extraction into an *n*-octanol phase as described by Socan *et al.* (see chapter 3.2.1.4).[40]

Variations

For the synthesis of [^{68}Ga]Ga-oxine, activity between 26–40 MBq of [^{68}Ga]$GaCl_3$ were applied. The first synthesis of [^{89}Zr]Zr-oxine was performed as described. Incubation was carried out for 60 min, before the formed complex was washed from cartridge using PBS and then repeated once. Further tested modifications were performed without the use of phosphate buffers during the complexation time. In addition, the formed complex was washed from the cartridge in several experiments already after only one incubation step (60 min) with a further charge of precursor solution 8-hydroxyquinoline (oxine, 0.3 ml) or with a different ethanolic solution (10% EtOH/H_2O, 50% EtOH/H_2O and 50% EtOH/PBS; 2 ml each, see chapter 4.1.2.2).

3.2.1.3. Man-Method

The kit formulation by Man *et al.*, published in 2020, focuses mainly on the synthesis of [^{89}Zr]Zr-oxine.[39] In the following, the method is referred to as Man-method or kit-method.

General procedure

For the synthesis of [^{68}Ga]Ga-oxine and [^{89}Zr]Zr-oxine by Man *et al.*, a precursor solution was prepared. First, 5 mg of 8-hydroxyquinoline were dissolved in ultrapure H_2O at 80 °C. The yellow solution was cooled down to r.t. before 2.38 mg HEPES was added and dissolved under shaking. In addition, 1 ml polysorbate 80 was added before the pH was adjusted to 7.9 with a 10 M NaOH. The solution was filled up to 10 ml with ultrapure water and stored in the dark.
For the experiments, 100 µl aliquots of this solution (containing 0.5 mg/ml oxine, 1 mol/L HEPES and 10 mg/ml polysorbate 80) were used. Samples of the radioactive precursor, [^{68}Ga]$GaCl_3$: 0.78–14.78 MBq and [^{89}Zr]Zr-oxalate: 1.3–12.5 MBq, were added to the aliquots with a maximum volume of 18 µl. For gallium-68 complexation, incubation time was 10 min, for zirconium-89 5 min at r.t. Radiochemical conversion was analysed *via* iTLC as reported by Man *et al.* (see chapter 3.2.1.4).[39]

Variations

For both complexations 2–18 µl [^{68}Ga]$GaCl_3$ or [^{89}Zr]Zr-oxalate were added to 100 µl precursor solution. Depending on the eluate activity, the applied activity varied between 0.78–14.78 MBq for gallium-68 complexes and 1.3–12.5 MBq for zirconium-89 complexes.

3.2.1.4. Quality Control

The radiochemical conversion (RCC) of the complexes synthesised according to all three protocols was determined *via* instant thin layer chromatography (iTLC). The RCC of the formed

[^{68}Ga]Ga-oxine or [^{89}Zr]Zr-oxine was evaluated by the percentage activity of the complex peak as a function of the total activity on the measured chromatogram. The plates were read with a radio TLC Scanner GITA Star or miniGita Dual and evaluated using the GINA STAR TLC software. For the syntheses according to Sinzinger *et al.*, the iTLC-method as described by Sinzinger was used. Here, 2.5 µl on *instant* TLC-SG paper was applied using 95% $CHCl_3$ and 5% MeOH as mobile phase. The $R_f = 0$ represents [^{68}Ga]$GaCl_3$ or colloids, while the $R_f = 1$ indicates the presence of the product [^{68}Ga]Ga-oxine.[89] The iTLC analysis to investigate the RCC of the complexes synthesised according to Socan *et al.* and Man *et al.* were performed as described by Man *et al*.[a] The samples of the complexes were analysed on Whatman® no.1. paper with 100% EtOAc as mobile phase. The $R_f = 0$ again represents the initial educts/colloids, the $R_f = 1$ the successful produced complexes [^{68}Ga]Ga-oxine and [^{89}Zr]Zr-oxine.[39]

In addition, the RCC was determined after the extraction into an organic phase (*n*-octanol) described by Man *et al.* Thereby, 10 µl radiotracer was added to a 1 ml mixture of pre-saturated *n*-octanol and PBS (1:1), then vortexed for 5 min before a short centrifugation was performed to achieve phase separation. The activity of each phase was determined *via* a gamma-counter.[39]

In the Socan variant, the yield was determined by measuring the remaining activity on the cartridge and the activity of the eluate as described by Socan *et al.* and expressed as percent rate (n.d.c.).[40]

Furthermore, the stability of the synthesised radiotracers in the crude matrix were investigated *via instant* thin layer chromatography over time.

3.2.2. Platelets Isolation/ Cell Culture

To label non-activated platelets, they first had to be isolated from the other blood components. To prevent activation of the platelets, the isolation steps must be carried out as gently as well as quickly as possible. Due to quicker isolation and better accessibility, various cell lines, such as PANC-1, AR42J and CHO K1, were also labelled instead of platelets. The isolation procedures are described first, before the labelling methods follow.

3.2.2.1. Platelets Isolation

First, 2 ml of anticoagulant citrate dextrose-A (ACD-A) was added to the Monovettes® to avoid clotting. Then 7 ml of blood was slowly drawn from an unclogged vein *via* a 21 g butterfly

[a] The analysis result of the iTLC is defined as radiochemical purity (RCP) by Man *et al.*

needle. The Monovettes® were carefully twisted twice before the blood was allowed to settle for about 10 min.[92]

In general, two different isolation protocols were used. The first described method was adapted from Sinzinger *et al.*[92], while the second is a protocol from a commercially available [^{111}In]In-oxine kit (in the following it is referred to as Curium-method)[93].

3.2.2.1.1. Sinzinger-Method

To remove the erythrocytes, the blood was centrifuged at 150 g for 10 min at r.t.. For a gentle separation, the brake was inactivated during all centrifugation steps. Afterwards, the supernatant PRP (platelet rich plasma) of two samples were pooled and centrifuged at 500 g for 10 min at r.t. Then, the supernatant PPP (platelet poor plasma) was removed and saved for later use. The cell pellet was resuspended in 1 ml cold Tyrode buffer (4 °C) or 0.9% NaCl with 15 vol.% ACD-A as required.[92]

3.2.2.1.2. Curium-Method

The blood was first centrifuged at 200 g for 15 min at r.t. The supernatant (PRP) was collected, two samples were pooled and mixed with 15 vol.% ACD-A before another centrifugation (640 g for 15 min r.t.) was performed to obtain a cell pellet. The PRP supernatant was saved for later use. The cells were resuspended in different buffer solutions depending on the experiment.[93]

3.2.2.2. Cell Culture

In addition to platelets, various cell lines as PANC-1 (pancreatic cancer cells), AR42J (pancreatic cancer cells) and CHO K1 (Chinese hamster ovarian cells) were used for labelling experiments. The cells were cultured in DMEM with 10% FBS, 1% L-glutamine solution and 1% P/S solution. The cell cultures were incubated under a moisture atmosphere containing 5% CO_2 at 37 °C. For the experiments detached cell suspensions in an approx. concentration of 0.1–7.2*10^6 cells/ml in PBS or 0.9% NaCl were used.

3.2.3. Cell Labelling

The stable platelets and cells obtained were labelled using the Sinzinger-method as well as the Curium-method. The general procedures for platelet labelling and a suitable adaptation for the cell lines PANC-1, CHO and AR42J are described followed by different modifications of the methods. In addition to [^{68}Ga]Ga-oxine and [^{89}Zr]Zr-oxine, labelling experiments with the [^{111}In]In-oxine were performed as proof of concept. Detailed tables, containing the most important parameters of all labelling experiments, can be found in the appendix (see

tables 30–37). Moreover, all labelling variants are provided with an individual code, where the letters in the first position stand for platelets (**P**) or cells (**C**), in the second position for the Sinzinger-method (**S**) or for the Curium-method (**C**), in the third position for gallium-68 oxine (**G**), for zirconium-89 oxine (**Z**) or for indium-111 oxine (**I**) and the letters in the fourth position for a consecutive numbering. The code system is used as abbreviation mainly in the results (see chapter 4.2).

3.2.3.1. Sinzinger-Method

General Procedure - Platelets

The radiotracer ([^{68}Ga]Ga-oxine or [^{111}In]In-oxine) was added in various activities and volumes to the isolated, stable platelets resuspended in cold Tyrode buffer. The suspension was incubated for 5 min at 37 °C without shaking. The previously obtained PPP was added to the suspension and the activity was measured *via* a dose calibrator. To remove the unbound gallium-68 or indium-111, the suspension was centrifuged at 500 g at 4 °C for 10 min with brake off. The two phases obtained were separated and the cell pellet was resuspended in Tyrode.[92] The activities were measured, and the labelling efficiency (LE) was determined *via* formula 1.[36]

$$LE\ [\%] = \frac{activity\ of\ cell\ fraction\ [MBq]}{activity\ of\ cell\ fraction\ [MBq] + activity\ of\ supernants\ [MBq]} \qquad (1)$$

Variations

Two different experiments of the Sinzinger-method for labelling stable platelets with [^{68}Ga]Ga-oxine were performed (see table 2). The parameters used for labelling with [^{111}In]In-oxine are also shown in table 2.

Table 2: Parameters used for the platelets labelling experiments via the Sinzinger-method.

Labelling-Parameter	[^{68}Ga]Ga-oxine A	[^{68}Ga]Ga-oxine B	[^{111}In]In-oxine
Code	PSGA	PSGB	PSIA
Buffer	Tyrode (4 °C)	Saline + 15% ACD-A	Tyrode (4 °C)
Labelling Activity [MBq]	3.7	2.3	0.05
V-Ratio (Cell Suspension:Tracer)	500:180	1000:360	1000:5
Time [min]	5	5	5
T [°C]	37	37	37
Shaker [rpm]	/	/	/
PPP-Addition [µl]	5.5 ml	5.5 ml	5.5 ml
n	1	2	1

General Procedure - Cells

A slightly modified version of the Sinzinger-method was only used once for labelling PANC-1 cells with [^{111}In]In-oxine. The radiotracer was added to the cell-saline-suspension and the mixture was then gently shaken for 5 min at 37 °C at 350 rpm. Afterwards, the cells were directly centrifuged (500 g, 4 °C, 10 min, brake off). The obtained phases were separated, the pellet was resuspended, and the activities were determined. The labelling efficiency was calculated *via* the formula 1. The parameters used are listed in table 3.

Table 3: Parameters used for the PANC-1 labelling experiments via the Sinzinger-method.

Labelling-Parameter	[^{111}In]In-oxine
Code	CSIA
Buffer	Saline
Cell Number / Suspension	$0.52*10^6$
Labelling Activity [kBq]	50
V-Ratio (Cell Suspension:Tracer)	1500:5
Time [min]	5
T [°C]	37
Shaker [rpm]	350
n	1

3.2.3.2. Curium-Method

General Procedure - Platelets

To prevent adsorption to synthesis materials, 0.4 vol.% Tris buffer was added to the [^{111}In]In-oxine solution in advance. The respective radiotracer was added in the desired activity and volume to the platelets resuspended in 1 ml saline. The suspension was left for 20 min at r.t. and shaken by hand from time to time. Then 667 µl PPP was added and the activity was measured. To remove free, unbound radiometals, a centrifugation step was performed at 1000 g for 15 min at r.t. with brake off. The phases obtained were separated, the cell pellet resuspended, and the activities measured. The labelling efficiency (LE) was determined *via* the measured activities (see formula 1).[93]

Variations

Various parameters, such as temperature, labelling activity or tracer volume, etc., were modified to achieve a possible increase in labelling efficiency. All the various modifications used for platelet labelling with gallium-68, zirconium-89 and indium-111-oxine are shown in table 4. Detailed informations of every individual experiment are listed in the appendix.

Table 4: Parameters used for the platelets labelling experiments via the Curium-method.

Labelling-Parameter	[^{68}Ga]Ga-oxine	[^{89}Zr]Zr-oxine	[^{111}In]In-oxine
Code	PCG	PCZ	PCI
Buffer	Saline PBS	PBS NaCl	Saline PBS ACD-A
Tris-Buffer	+ 0.4 vol.% /	/	+ 0.4 vol.%
Labelling Activity [MBq]	0.16–1.3	0.06–3.31	0.02–1.7
Tracer volume [µl]	25–300	25	1.5–600 58 µl in 942 µl Saline
Time [min]	20	20	20
T [°C]	r.t. 37	r.t. 37	r.t.
Shaker [rpm]	0–300	0–300	0–300 hand
PPP-Addition [µl]	667 /	667 /	667

General Procedure - Cells

The cell lines PANC-1, AR42J and CHO K1 were also resuspended in 1 ml saline and incubated with the respective tracer in various activities and volumes for 20 min at r.t.. After a centrifugation step (1000 g, 15 min, r.t., brake off), the measurement of the activities of both separated phases, as well as the calculation of the resulting labelling efficiency (see formula 1) followed.

Variations

The basis for the *in vitro* cell labelling (PANC-1, AR42J and CHO K1 cell lines) was the Curium-method with changed parameters. A summary of the different variants is shown in table 5.

Table 5: Parameters used for the PANC-1/ AR42J/ CHO K1 cell labelling experiments via the Curium-method.

Labelling-Parameter	[^{68}Ga]Ga-oxine	[^{89}Zr]Zr-oxine	[^{111}In]In-oxine
Code	CCG	CCZ	CCI
Buffer	PBS	PBS	Saline PBS
Cell Number/Suspension	$5.7*10^5$–$7.2*10^6$	1.3–$3.4*10^6$	0.13–$1.7*10^6$
Tris-Buffer	/	/	+ 0.4 vol.%
Labelling Activity [MBq]	0.25–6.0	0.02–0.70	0.03–1.06
V-Ratio (Cell Suspension:Tracer)	10:1–1:1.3	1000:25 1000:30	40:1–2:1
Time [min]	10 15 20	15 20	15 20
T [°C]	r.t. 37	r.t. 37	r.t. 37
Shaker [rpm]	350–750	hand 450– 650	hand 400–650

4. Results

4.1. Radiotracer-Syntheses

4.1.1. Radiosyntheses Results according to the Sinzinger-Method (Pot-Method) and Modifications

4.1.1.1. [^{68}Ga]Ga-oxine: Results

A total of eleven syntheses were carried out *via* the Sinzinger SOP. The results are described in table 6. Eight syntheses were successfully performed after 15 min reaction time (t_0) with a mean value of 90 ± 13% conversion measured by radio-TLC of the crude mixture, while in three reactions (010, 012; 014) no complex formation could be detected after 15 min. Figure 3 shows the iTLC analysis of the initial radioprecursor [^{68}Ga]$GaCl_3$ (R_f = 0; **A**), and in comparison the iTLC chromatogram of [^{68}Ga]Ga-oxine (R_f = 1; **B**; experiment 011).

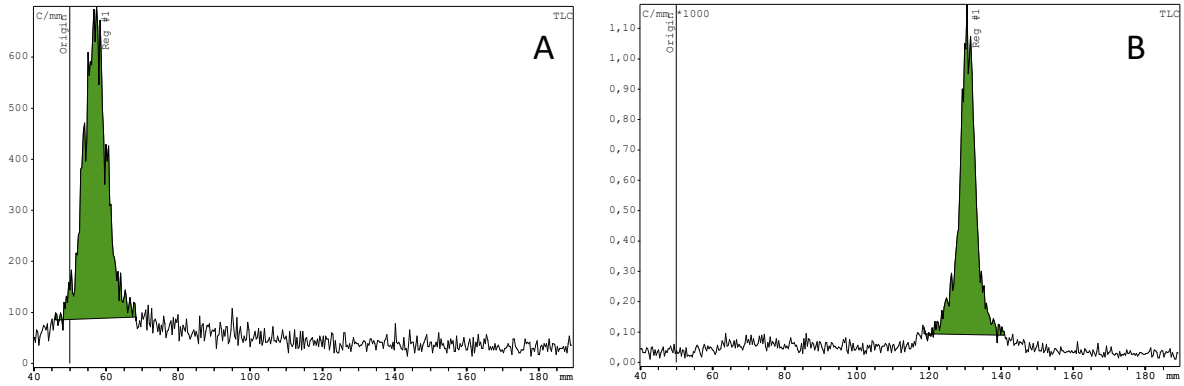

*Figure 3: iTLC-chromatograms of the initial radio precursor [^{68}Ga]$GaCl_3$ at R_f = 0 (**A**) and of the [^{68}Ga]Ga-oxine complex synthesised via the Sinzinger-method at R_f = 1 (**B**).*

In two experiments (SOPI010 and 012) the complex formation could only be detected after a further 60 min reaction time after preparation, with > 99% (010; see figure 4) and 86% (012) yield, respectively.

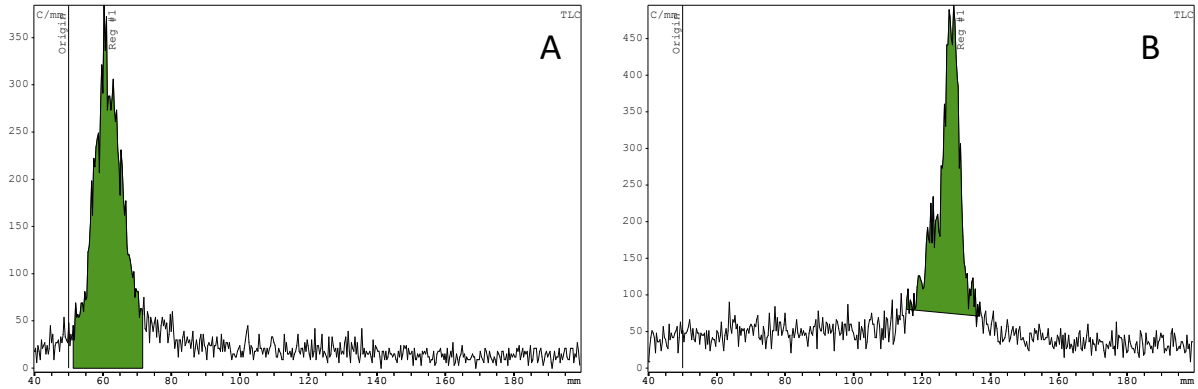

*Figure 4: iTLC chromatograms of SOPI010 after 15 min incubation (t_0) with no radiochemical conversion (RCC) (**A**) and after 60 min post-synthesis with > 99% RCC (**B**).*

In experiment SOPI014a, no complexation could be analysed *via* iTLC measurements even after 90 min additional incubation time (measuring points: t_0 = 0 min, t_1 = 45 min, t_2 = 90 min after preparation). But *via n*-octanol extraction, complex formation could be detected 30 min post-synthesis yielding 98%.

Overall, the extraction of the formed complex into the organic phase was carried out in six independent experiments, resulting in a mean radiochemical conversion of 86 ± 15% (see table 6).

Table 6: Synthesis results of the experiments performed according to the SOP of Sinzinger et al. including the activities used and the mean values with standard deviations.

Sinzinger-method [^{68}Ga]Ga-oxine	Activity applied [MBq]	RCC (iTLC) [%]	RCC (Extraction) [%]
SOPI007	20.00	93	n.p.
SOPI009	8.35	> 99	n.p.
SOPI010	9.11	*	n.p.
SOPI011	9.15	> 99	n.p.
SOPI012	12.00	*	n.p.
SOPI014a	8.89	0	98
SOPI015a	8.26	87	94
SOPI016a	9.40	> 99	96
SOPI017a	8.77	68	66
SOPI018a	7.85	72	67
SOPI019a	9.53	> 99	98
Mean value ± Standard deviation		90 ± 13** (n = 8)	86 ± 15 (n = 6)

**Complexation was only achieved after 75 min. **Mean value and standard deviation of all successful syntheses after 15 min.*

In general, activities in the range of 2.0–20.0 MBq of [^{68}Ga]$GaCl_3$ were used (see table 6). The pH value of the reaction solution was between 4.5–5.0.

Variations

The synthesis protocol according to Sinzinger *et al.* was modified *via* two different approaches resulting in a change of the pH value of the reaction solution.

Variation M

First, the pH value of 4.5–5.0 was lowered by changing the concentration of the sodium acetate solution (SOPI014, 018 and 019). Therefore, a 1 M NaOAc (in the following referred to 1M-method), resulting in a pH range of 0.0–1.0, as well as a 2 M solution (pH = 1.0-1.5; 2M-method) were used instead of the saturated solution. The mean values of the iTLC and *n*-octanol extraction results are shown in table 7. The experiments using 1 M NaOAc (SOPI014b,

18b and 19b) yielded a mean conversion rate of 22 ± 4% for the iTLC analyses and 7 ± 4% for the extraction experiments. For the 2M-method (SOPI014c, 18c and 19c), an iTLC mean of 40 ± 10% yield was calculated, while the mean value of the RCC *via* extraction was 23 ± 7%.

Table 7: Mean values and standard deviations of the RCC via iTLC and via n-octanol extraction of the experiments performed according to the SOP of Sinzinger et al. and of the variation M.

	Sinzinger	1M	2M
RCC (iTLC) [%]	90 ± 13 (n = 8)	22 ± 4 (n = 3)	40 ± 10 (n = 3)
RCC (Extraction) [%]	86 ± 15 (n = 6)	7 ± 4 (n = 3)	23 ± 7 (n = 3)

Variation V

In the second approach, the volume of the sat. NaOAc solution was increased resulting in a higher pH of the reaction solution (Sinzinger*/1V: pH = 5.5–6.0; 2V: pH = 7.5–8.0). The results are shown in table 8. Using the Sinzinger*/1V-method, an iTLC mean of 94 ± 8% RCC and an extraction mean of 89 ± 9% RCC were obtained. The mean value of the iTLC measurements obtained by the 2V-method was 96 ± 4% radiochemical conversion, whereas the one of the extraction measurements was 92 ± 6% RCC.

Table 8: Mean values and standard deviations of the RCC via iTLC and via n-octanol extraction of the experiments performed according to the SOP of Sinzinger et al. and of the variation V.

	Sinzinger	Sinzinger*/1V	2V
RCC (iTLC) [%]	90 ± 13 (n = 8)	94 ± 8 (n = 3)	96 ± 4 (n = 3)
RCC (Extraction) [%]	86 ± 15 (n = 6)	89 ± 9 (n = 3)	92 ± 6 (n = 3)

Results of Sinzinger*/1V

The optimised version Sinzinger*/1V was adopted for further experiments within the activity range of 8.4–10.0 MBq. In summary, the results are shown in table 9. Extraction into an organic phase (*n*-octanol) was only carried out in the optimisation experiments. In total, nine syntheses were performed *via* the modified Sinzinger*/1V protocol with an iTLC mean value of 94 ± 6% conversion rate.

Table 9: Synthesis results of the experiments performed via the modified Sinzinger/1V protocol including the activities used and the mean values with standard deviations.*

Sinzinger*/1V [^{68}Ga]Ga-oxine	Activity applied [MBq]	RCC (iTLC) [%]	RCC (Extraction) [%]
SOPI015b	8.4	> 99	93
SOPI016b	9.4	> 99	97
SOPI017b	8.7	85	79
SOPI022	9.0	98	n.p.
SOPI026	9.4	> 99	n.p.
SOPI033	9.0	90	n.p.
	9.0	85	n.p.
SOPI058	10.0	96	n.p.
SOPI059	10.0	94	n.p.
Mean value ± Standard deviation		94 ± 6 (n = 9)	89 ± 9 (n = 3)

In experiment SOPI022, 0.4 vol.% Tris buffer was added to the reaction mixture following the commercial labelling variant of the [^{111}In]In-oxine kit, yielding 98% RCC. The integrated green area indicates the origin as well as the presence of [^{68}Ga]$GaCl_3$/colloid (R_f = 0), the integrated red area illustrates the formed complex (R_f = 1). Chromatogram **B** (gallium-68 complex with 0.4% Tris buffer) was obtained two hours after the analysis of **A** (see figure 5).

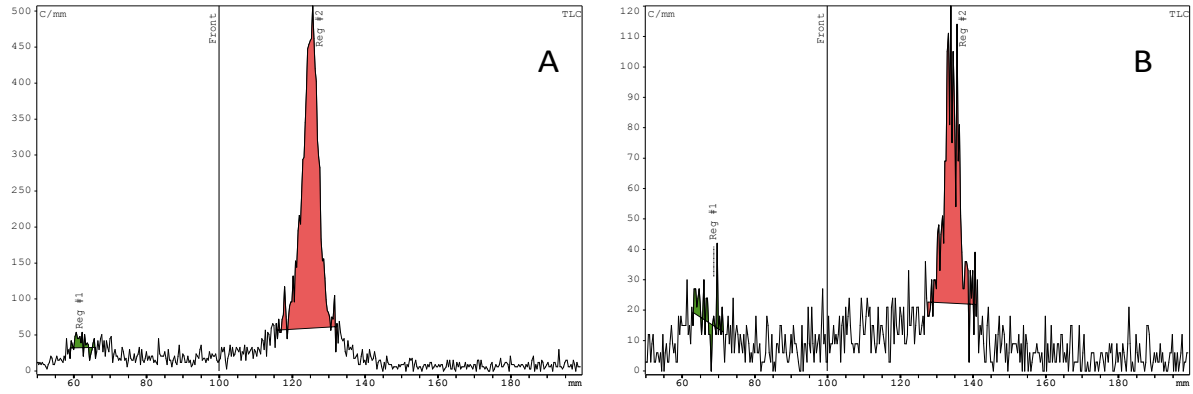

*Figure 5: iTLC chromatograms of [^{68}Ga]Ga-oxine after 15 min incubation (t_0) with 98% conversion rate (**A**) and of [^{68}Ga]Ga-oxine + 0.4 vol.% Tris-buffer 120 min post-synthesis with > 94% conversion rate (**B;** SOPI022). The front mark in the chromatograms has no relevance in relation to these measurements - the chromatograms were developed until shortly after the red-integrated area.*

Stability Measurements of the Sinzinger-Method:

iTLC measurements were used to investigate the stability of the radiotracers in the crude matrix over time. The results of the stability measurements of the synthesised gallium-68 tracers according to Sinzinger *et al.* are shown in figure 6.

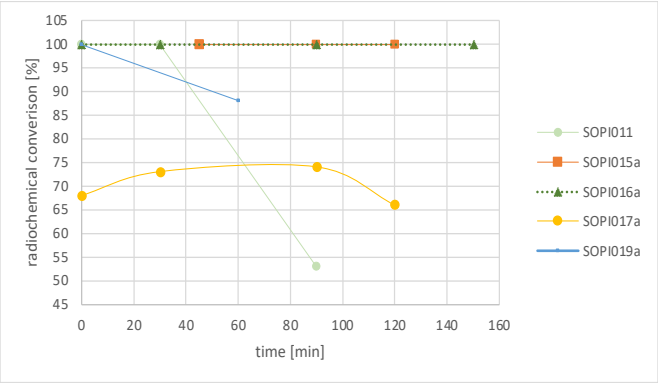

Figure 6: Stability profiles of the [^{68}Ga]Ga-oxine produced according to Sinzinger as a function of time in the crude mixture.

Stability in the crude matrix and initial RCC varied between the gallium-68 oxine replicates, as illustrated in figure 6: SOPI015a and 016a showed stable patterns. The product of experiment 017a, showed a lower conversion but stability over time. SOPI011 was stable for 30 min post-synthesis before the complex dissociated (~50%). For 019a, the RCC decreased by 12% after 60 min. Accordingly, different stability patterns were obtained for the complexes synthesised according to Sinzinger *et al*.

In comparison, the modified complexes of the variation V (Sinzinger*/1V and 2V-variant) showed overall good, consistent stability profiles in the crude mixture (see figure 7). The stability pattern of the gallium-68 complexes of 015b and 017b (Sinzinger*/1V) appeared to show a slight tendency to decrease over the 120 min period, while the values of complexes 015c and 017c (2V) varied a little. However, all values were within a small percentage range, indicating good stability patterns.

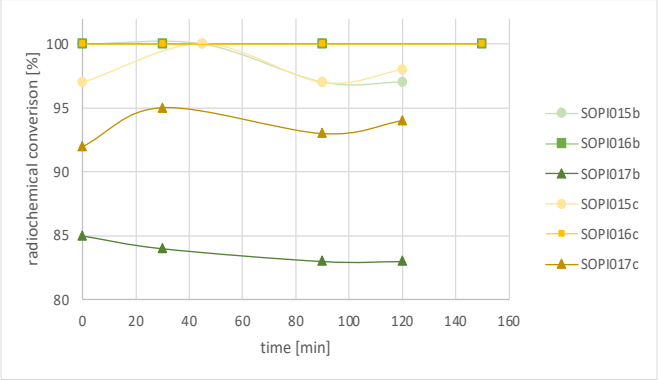

Figure 7: Stability profiles of the [^{68}Ga]Ga-oxine produced according to Sinzinger/1V (b, green) and 2V (c, yellow) as a function of time.*

4.1.2. Radiosyntheses Results according to the Socan-Method (Cartridge-Method) and Modifications

4.1.2.1. [^{68}Ga]Ga-oxine: Results

A total of thirteen syntheses of [^{68}Ga]Ga-oxine, according to Socan *et al.* with activities between 26–40 MBq of [^{68}Ga]$GaCl_3$ without any modifications of the protocol, were carried out. The averaged loading efficiency

of the cartridge in all thirteen experiments was 94 ± 3%. The mean value of the yield was 16 ± 4%. In three syntheses no organic complex was detected and are therefore excluded as fail syntheses from the presented results.

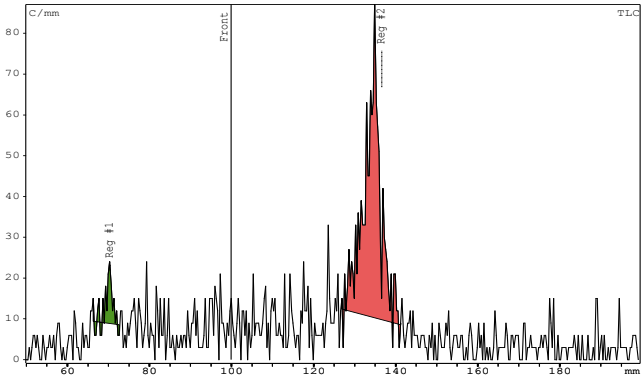

Figure 8: iTLC chromatogram of [^{68}Ga]Ga-oxine with about 93% complex formation (SOPI048).

The mean value of the radiochemical purity of the successful syntheses was 94 ± 4% (n = 10) *via* iTLC analysis. In five experiments the complex formation was also investigated after an *n*-octanol extraction, leading to 95 ± 2% (see table 10). Figure 8 shows a representative iTLC analyses of experiment SOPI048 with a purity of approx. 93%. The applied activities, as well as all synthesis results, are shown in table 10. In all experiments, the pH of the PBS eluate was 7.5, except for the unsuccessful synthesis, experiment SOPI037, where the pH was 8.0.

Table 10: Synthesis results of the experiments performed according to Socan et al. including the activities used and the mean values with standard deviations.

Socan [^{68}Ga]Ga-oxine	Activity applied [MBq]	LoE [%]	Yield [%]	RCP (iTLC) [%]	RCP (Extraction) [%]
SOPI037	29.99	95	9	*	n.p.
SOPI038	28.21	95	17	> 99	94
SOPI040	26.42	95	13	> 99	97
SOPI042	38.64	85	11	92	93
SOPI043	37.72	93	22	96	94
SOPI044	38.13	95	19	94	97
SOPI048	39.99	95	15	93	n.p.
SOPI049	37.13	94	18	94	n.p.
SOPI053	36.62	89	13	89	n.p.
SOPI054	38.80	97	21	84	n.p.
SOPI055	38.07	97	20	*	n.p.
SOPI056	37.06	95	15	*	n.p.
SOPI057	40.04	95	16	98	n.p.
Mean value ± Standard deviation		94 ± 3 (n = 13)	16 ± 4 (n = 13)	94 ± 4** (n = 10)	95 ± 2 (n = 5)

**No complex formation could be detected. **Mean value and standard deviation of all successful syntheses.*

Table 11 shows the synthesis parameters and the results reported by Socan *et al.* in comparison with those of the experiments carried out according to the protocol. Since Socan *et al*. postulated an independence of the volume of the sodium acetate solution (c = 155 mg/ml), and consequently a pH independence,[40] the volume of the base was standardised to 1 ml. Both the measured pH values of the loading solutions and the loading efficiencies (LoE) of the cartridge obtained are in a similar range as reported by Socan *et al.* However, the mean yield of the syntheses differs from those of Socan *et al.* by more than half (50 vs. 16 %). On the other hand, the radiochemical purity analysed after extraction was found to be slightly improved from the reported values of Socan *et al*. The measured pH values of the products vary considerably. While the elution of the gallium-68 complexes with PBS resulted in pH of 7.5, Socan *et al.* are reporting decreased pH of 5.9 ± 0.9.[40]

Table 11: Comparison between the parameters and results reported by Socan et al.[40] and the performed experiments SOPIxxx according to Socan.

[^{68}Ga]Ga-oxine	Reported values[40]	SOPIxxx acc. to Socan
Activity applied [MBq]	10–50	26–40
$V_{(NaOAc)}$ [ml]	0.5–5	1
$pH_{(loading\ solution)}$	4–6	4.5–5.5
LoE [%]	96 ± 3 (n = 25)	94 ± 3 (n = 13)
Yield [%]	50 ± 12 (n = 18)	16 ± 4 (n = 13)
$pH_{(product)}$	5.9 ± 0.9 (n = 18)	7.5 (n = 12)
RCP (iTLC) [%]	n.p.	94 ± 4 (n = 10)
RCP (Extraction) [%]	94 ± 7 (n = 18)	95 ± 2 (n = 5)

In a further experiment, SOPI038, further PBS-elutions were carried out to increase the yield, as is reported by Socan *et al.* for other radionuclides.[40] Therefore, the efficiency of the subsequent elutions was investigated by measuring the eluted activity of five elutions. With all five elutions, a yield of 40% was achieved (see table 12), and reached much closer the reported average yield of 50 ± 12%.[40]

Table 12: Elution efficiencies [%] of the five elutions performed in experiment SOPI038.

#	$Activity_{(cartridge)}$ [MBq]	$Activity_{(eluate)}$ [MBq]	Efficiency [%]
1	12.46	2.50	17
2	8.77	0.96	10
3	7.99	0.63	7
4	7.23	0.30	4
5	6.87	0.12	2
Σ (n = 5)		4.51	40

However, other attempts were made to improve the yield by changing other factors. For example, various small adjustments in handling were made to keep the processing time as short as possible, but no improved result than 22% RCP could be achieved (see table 10).

4.1.2.2. [^{89}Zr]Zr-oxine: Results

In contrast to the gallium-68 oxine synthesis, the Socan protocol as originally described was only performed in one [^{89}Zr]Zr-oxine-experiment (SOPI066b), resulting in a 24% yield with a 93% radiochemical purity (RCP) for the first complex elution and in an additional 10% yield with a 17% RCP for the second eluate. In all further experiments, a second incubation step after a PBS elution was omitted. Furthermore, instead of a PBS solution as eluent, another precursor solution (pH = 5.0, V = 0.3 ml) as well as different ethanolic solutions (pH = 7.0–7.5,

V = 2 ml), were used to obtain the complex. The synthesis of [^{89}Zr]Zr-oxine was carried out eight times with various modifications of the protocol. As shown in table 13, a loading efficiency of at least 99% was achieved in all eight experiments. The yields and RCP values obtained differ depending on the modification.

Table 13: Synthesis results of the experiments performed according to Socan et al. including the activities used as well as the eluent used to obtain [^{89}Zr]Zr-oxine.

Socan [^{89}Zr]Zr-oxine	#	Activity applied [MBq]	Eluent	LoE [%]	Yield [%]	RCP (iTLC) [%]
SOPI066b	1	3.08*	PBS	> 99	24 & 10	93** & 17**
SOPI067b	1	3.07*	Oxine / PBS	> 99	54 & 7	96 & n.p.
SOPI068b	1	2.04	Oxine	> 99	60	98
	2	2.03	PBS	> 99	33	47**
	3	2.01	10% EtOH/H_2O	> 99	28	83
SOPI070b	1	2.05	Oxine	99	76	70***
	2	2.06	50% EtOH/PBS	> 99	64	64
	3	2.04	50% EtOH/H_2O	99	75	n.p.

**The activity was measured via a dose calibrator calibrated for indium-111. **The activities of the developed thin layer plate-parts were gamma counted to obtain the RCP. ***The chromatogram showed a typical pattern for this development length – a fronting of the product, so a higher conversion can be assumed[39].*

A comparison between the parameters and results reported by Socan and those obtained in the experiments according to Socan *et al.* are given in table 14. For comparison reasons, only the results of the first PBS elution were considered, resulting in 29 ± 5% (n = 2) yield, whereas the values reported in the literature were obtained from two elutions with a mean value of 64 ± 9% (n = 8).[40] The reported radiochemical purity by Socan was 93 ± 6% (*via* organic extraction)[40], while 47% and 93% RCP (*via* iTLC) were obtained in the two experiments performed.

Table 14: Comparison between the parameters and results reported by Socan et al.[40] and the performed experiments SOPIxxx according to Socan.

[^{89}Zr]Zr-oxine	Reported Values[40]	SOPIxxx acc. to Socan
Activity applied [MBq]	2–3	2.0–2.1
$V_{(NaOAc)}$ [ml]	0.2–0.3	0.25–0.3
$pH_{(loading\ solution)}$	5–5.3	6–7
LoE [%]	96 ± 3 (n = 2)	100 ± 1 (n = 8)
Yield [%]	64 ± 9 (n = 8)	29 ± 5 (n = 2)
$pH_{(product=PBS\text{-}eluate)}$	7.9 ± 0.6 (n = 8)	7.4 (n = 2)
RCP [%] (PBS)	93 ± 6 (n = 8)	range: 47–93 (n = 2)

Based on these results, an alternative eluent was sought (see table 13). In the first modified approach 067b, the cartridge was loaded with another oxine solution (V = 300 µl) after 60 min

incubation without prior elution with PBS. The resulting first fraction yielded 54% of the total activity and RCP of 96% (for chromatogram see figure 17 in appendix). After a further incubation time of 60 min, about 7% of the remaining activity (based on the total activity present after the first elution) was washed off the column using 2 ml PBS. A radiochemical purity determination of the second fraction was not carried out.

For 068b, three experiments using various eluents were carried out simultaneously: 60% of the total activity with 98% RCP was obtained in 068b1 (oxine & PBS) (for chromatogram see figure 18 in appendix). 33% of the total activity with 47% complex formation was eluted *via* PBS (068b2) and 28% of the activity with 83% RCP was eluted in 068b3 (see table 13). The spotted activity on the TLC plate of the latter two experiments was too low for an accurate distinction and evaluation *via* iTLC scanner. Accordingly, the developed TLC plates were divided into a reactant and product part to measure the activity of each part *via* a gamma counter.

In approach 070b, the ethanol content of all eluents was increased to 50%. In 070b1 (oxine), 76% of the total activity was washed off the column with a 70% complex formation. 070b2 (50% EtOH in EtOH) yielded 64% elution, showing 64% RCP (for chromatograms see figure 19 in appendix). 75% of the total activity was obtained eluting with the H_2O:EtOH solution (070b3), but no complex formation was observed *via* iTLC measurements.

In total, the complex was successfully synthesised *via* a new precursor loading in three different approaches. Table 15 shows the results of these experiments with a mean yield of 63 ± 11% (n = 3) and a mean radiochemical purity of 88 ± 16% (n = 3). In 068b1, 60% yield with 98% RCP was achieved, representing the best result of the [^{89}Zr]Zr-oxine experiments carried out according to the cartridge-method.

Table 15: Synthesis results of the [^{89}Zr]Zr-oxine-experiments performed according to Socan et al. via oxine-elution including the mean values with standard deviations.

Socan [^{89}Zr]Zr-oxine	Yield [%]	RCP [%]
SOPI067b1	54	96
SOPI068b1	60	98
SOPI070b1	76	70*
Mean value ± Standard deviation	63 ± 11 (n = 3)	88 ± 16 (n = 3)

**The chromatogram showed a typical pattern for this development length – a fronting of the product, so a higher yield can be assumed.[39]*

In addition, the stabilities of the successful syntheses in the crude matrix according to Socan *et al.* were analysed two days post-synthesis (t_1 = 48 h). Figure 9 shows the iTLC scans of zirconium-89 oxine immediately after the synthesis (t_0 = 0 min; **A** & **C**) compared to those at t_1 (**B** & **D**). While the complex in the precursor solution seems stable (**A** & **B**), the complex obtained in the EtOH:PBS crude matrix has already completely decomposed after two days (see figure 9**D**).

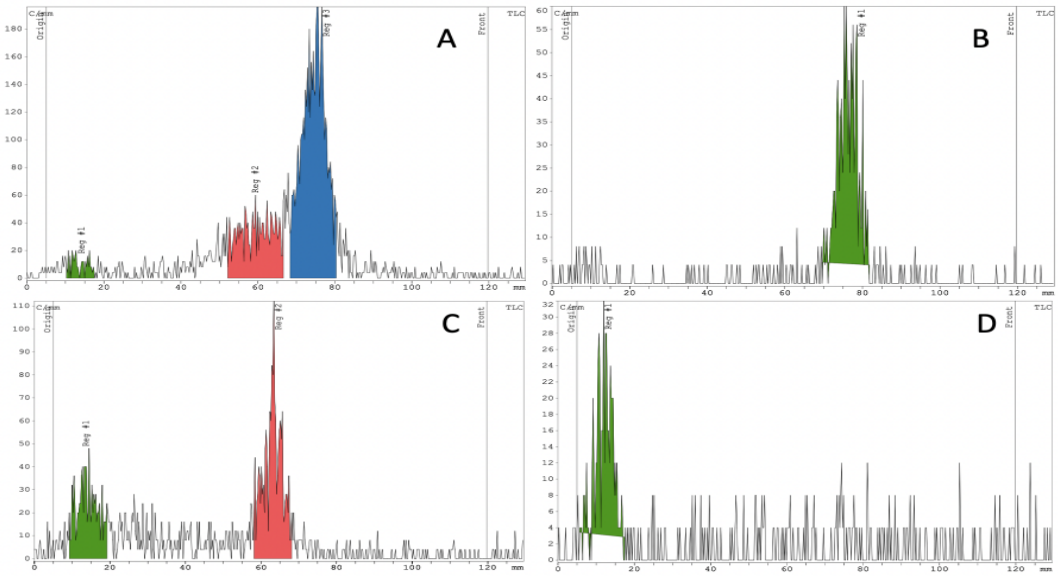

*Figure 9: Stability measurements of SOPI070b1 directly after synthesis (t_0) with about > 70% complex formation (**A**), after 48 h post-synthesis (t_1) with > 99% complex formation (**B**) and of SOPI070b2 directly after synthesis (t_0) with about 64% complex formation (**C**) and after 48 h post-synthesis (t_1) with no complex formation (**D**).*

4.1.3. Radiosyntheses Results according to the Man-Method (Kit-Method)

The Man-method synthesising the metal complexes in a more basic matrix formulation was also carried out for [^{68}Ga]Ga-oxine and [^{89}Zr]Zr-oxine. The parameters for the kit method are described in more detail in chapter 3.2.1.3.

4.1.3.1. [^{68}Ga]Ga-oxine: Results

In total, the protocol according to Man *et al.* was applied seven times to synthesise the gallium-68 complex, resulting in a mean value of 96 ± 7% (n = 7) radiochemical conversion (see table 16). The pH value was 8.5 in all syntheses and the reaction time was 10 min.

Table 16: Synthesis results of the [^{68}Ga]Ga-oxine-experiments performed according to Man et al. including the mean yield with standard deviations.

Man [^{68}Ga]Ga-oxine	Activity applied [MBq]	RCC [%]
SOPI060	4.68	> 99
SOPI061	4.60	> 99
SOPI062	14.78	> 99
SOPI063a	4.54	> 99
SOPI063b	4.59	> 99
SOPI082a	0.78	88
SOPI082b	0.78	82
Mean value ± Standard deviation		96 ± 7 (n = 7)

4.1.3.2. [^{89}Zr]Zr-oxine: Results

[^{89}Zr]Zr-oxine was also synthesised according to the kit formulation of Man *et al*. In total, thirteen experiments were performed, achieving a mean radiochemical conversion of 97 ± 2% (n = 10). The reaction time was 10 min and the pH value was 8.5. In table 17 the obtained results are shown.

Table 17: Synthesis results of the [^{89}Zr]Zr-oxine-experiments performed according to Man et al. including the mean yield with standard deviation.

Man [^{89}Zr]Zr-oxine	Volume [^{89}Zr]Zr-oxalate [µl]	Activity applied [MBq]	RCC [%]
SOPI066c	2	3.3*	> 99
SOPI068c	4	2.0	> 99
SOPI070c	5	1.6	93
SOPI071b	10	2.8	> 99
SOPI079b	2	2.0	96
SOPI080	4	2.0	98
SOPI083	2	2.0	99
SOPI084	18	12.5	97
SOPI085b	18	2.6	> 99
SOPI086	18	1.3	95
Mean value ± Standard deviation			97 ± 2 (n = 10)

**The activity was measured via a dose calibrator calibrated for indium-111.*

Figure 10 illustrates the iTLC result of approach 079b, as a representative example with a 96% RCC.

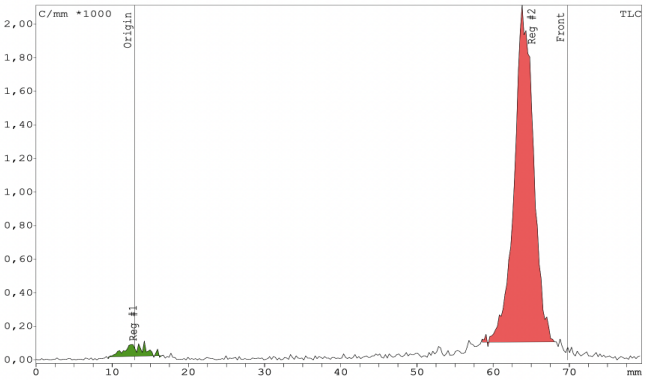

Figure 10: iTLC chromatograms of SOPIO79b with about 96% complex formation.

In addition, the stability of zirconium-89 oxine in the crude matrix was measured for up to seven days. Figure 11 shows four chromatograms of four different time points (0 h–24 h–48 h–7 d) of experiment 083. The complex remained relatively stable during this time. 90% RCC were still measured after seven days.

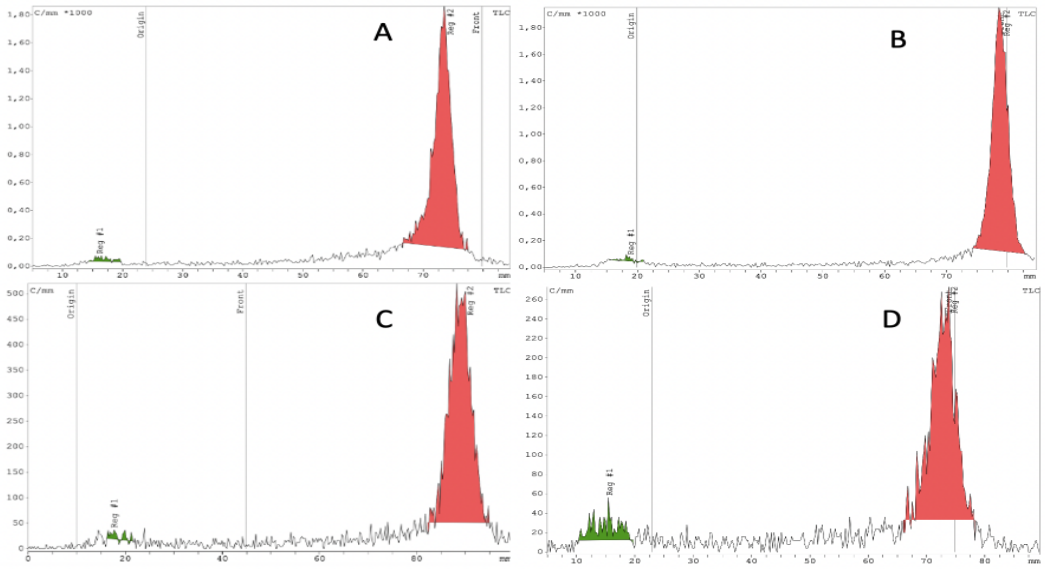

*Figure 11: Stability measurements of SOPI083 directly after synthesis (t_0) with 99% complex formation (**A**), after 24 h post-synthesis with 99% complex formation (**B**), after 48 h post-synthesis with 99 % complex formation (**C**) and after 7 d post-synthesis (t_1) with 90 % (**D**).*

4.2. Platelet Isolation/ Cell Culture

In all experiments, a visible cell pellet was obtained, and the platelets have not been visibly activated.[b] The number and the viability of the isolated platelets were examined using a hemocytometer (Neubauer counting chamber) or an automatic cell counter, leading to an approximate range of 270.000–410.000 platelets per µl, depending on the individual blood donor. In addition various cells, mainly from the PANC-1 cell line, were labelled with the produced gallium and zirconium tracers and with the commercially available and established radiotracer [^{111}In]In-oxine for cell labelling to improve the protocol by various modifications. The results of the labelling experiments carried out as well as their most relevant parameters are shown in the tables below. In addition, tables with all applied parameters of the individual experiments can be found in the appendix (see tables 30–37). In the first column of all tables, the labelling conditions described by Sinzinger or Curium, respectively, are highlighted in dark yellow. Experiments performed under the described conditions are highlighted in light yellow.

4.2.1. Platelets and Cell Labelling using the Sinzinger-Method

After the appropriate centrifugation steps, *via* the Sinzinger-method, approximately 3.5–5.5 ml of platelet-poor plasma (PPP) was separated from the cell pellet, platelet-rich plasma

[b] In the appendix, figure 20 displays an activation of platelets in comparison with non-activated, resuspended platelets.

(PRP), coming from two pooled Monovettes®. The volume of PPP varied depending on the blood donor.

For the two labelling experiments only [^{68}Ga]Ga-oxine with at least ≥ 93% RCC was used. In experiment SOPI010, the labelling protocol of Sinzinger *et al.* was performed without any modifications, resulting in 1% cell labelling efficiency (LE) (**PSGA**). In SOPI007, the cold Tyrode solution was replaced by a 0.9% NaCl + 15% ACD-A solution, leading to a 1% (n = 2) LE (**PSGB**). In the proof of concept using [^{111}In]In-oxine tracer, the LE was up to 15% (**PSIA**, see table 18 and 30).

Table 18: Results and parameters used of the platelet labelling experiments performed according to Sinzinger et al. The standard parameters of the protocol are highlighted in dark yellow.

Experiment	Code	Tracer	Buffer	Labelling Activity [MBq]	V-Ratio	LE [%]
SOPIxxx	PS	[^{111}In]In-oxine	Tyrode (4°C)	n.r.	n.r.	n.r.
SOPI010	PSGA	[^{68}Ga]Ga-oxine	Tyrode (4°C)	3.7	1000:360	1
SOPI007	PSGB	[^{68}Ga]Ga-oxine	Saline + 15% ACD-A	2.3	500:180	1 ± 0 (n = 2)
SOPI020a	PSIA	[^{111}In]In-oxine	Tyrode (4°C)	0.05	1000:5	15

In addition, one in vitro cell labelling experiment, 020c, using [^{111}In]In-oxine was also conducted, resulting in 10% LE (**CSIA**, see table 3 and 31).

In both indium-111 oxine experiments, the recommended Tris buffer (0.4 vol.%), which prevents adsorption to the plastic vessels or syringe of the lipophilic tracer, was not added to follow the Sinzinger protocol. Since the labelling experiments with [^{111}In]In-oxine also achieved low labelling efficiencies in both platelets and PANC-1 cells, different isolation and labelling protocol was applied in the following experiments.

4.2.2. Cell Labelling Method according to the Curium-method

In total, the labelling experiments were carried out with three different radiotracers using the Curium-method. For a better overview, the labelling conditions described by Curium are in the first column of all tables, highlighted in yellow.

4.2.2.1. Labelling Cells using [^{111}In]In-oxine

Labelling of Cells

Eleven modifications of the Curium-protocol were performed for cell labelling using [^{111}In]In-oxine (see table 32 for details).

In table 19, the results of the modifications **CCIA**–**CCIC** with different volumes, activities and cell numbers are shown. The results varied between 14 and 76% LE, indicating a certain influence by the cell number and by the volume ratio. Accordingly, the next labelling variations **CCIE**–**CCIF** were performed at higher cell numbers, while the ratio of the volumes was varied, at comparable activities. In addition, PBS was chosen instead of saline. The **CCID**-**CCIF** experiments showed an increased LE by enhancing the tracer volume (see table 20).

Table 19: Results and parameters used of PANC-1 labelling experiments performed according to the Curium-method using [^{111}In]In-oxine as radiotracer. The standard parameters of the protocol are highlighted in dark yellow.

Experiment	CODE	Buffer	Cell number *10^6	Labelling Activity [MBq]	V-Ratio	LE [%]
SOPIxxx	CCI	Saline	n.r.	4–37 M	n.r.	n.r.
SOPI023b	CCIA	Saline	0.15	0.74–0.75	1000:215	76 ± 0.5 (n = 3)
SOPI023b	CCIB	Saline	0.15	0.17	1000:50	62
SOPI024b	CCIC	Saline	0.12	0.3, 0.4	1000:500	14 ± 0 (n = 2)
SOPI029b	CCID	PBS	0.14-0.19	1.03–1.06	8:1	61 ± 4 (n = 6)
SOPI029b	CCIE	PBS	0.14-0.19	1.03–1.06	4:1	71 ± 7 (n = 6)
SOPI029b	CCIF	PBS	0.19	1.01, 1.03	2:1	82 ± 1 (n = 2)

In the experiments in table 21, the incubation conditions were changed. The incubation of SOPI030b (**CCIG**, **CCIH**) was carried out at 400 rpm. The volume ratios, as well as the activities, were obtained from the remaining batch of [^{111}In]In-oxine + 0.4 vol.% Tris buffer, resulting in low volume ratios. With a comparable volume ratio to **CCID**, a similar result was received with **CCIG** (despite different incubation parameters). In addition, the result of **CCIH** was accordingly lower at a lower volume.

Further changes in the incubation conditions were made in experiment 075b. In addition, the volume of the tracer was reduced even further to 25 µl, while the cell number was increased. The changes resulted in a lower mean value (34%, **CCII**).

Table 20: Results and parameters used of PANC-1 labelling experiments performed according to the Curium-method using [^{111}In]In-oxine as radiotracer. The standard parameters of the protocol are highlighted in dark yellow.

Experiment	CODE	Cell number *10^6	Labelling Activity [MBq]	V-Ratio	Time [min]	T [°C]	Shaker [rpm]	LE [%]
SOPIxxx	CCI	n.r.	4–37	n.r.	20	r.t.	/	n.r.
SOPI030b	CCIG	0.16	0.52	400:55	20	r.t.	400	61
SOPI030b	CCIH	0.16	0.89, 0.90	400:35	20	r.t.	400	range 41–58 (n = 2)
SOPI075b	CCII	1.65	0.17–0.27	1000:25	20	37	650	34 ± 2 (n = 5)

In table 21, the influence on the labelling efficiency of different cell lines is illustrated. Cells of four different cell lines were resuspended in PBS and incubated at a 1:1 ratio with [^{111}In]In-oxine. All LE obtained were within a similar range, indicating independence of the cell lines.

Table 21: Results and parameters used of cell labelling experiments performed according to the Curium-method using [^{111}In]In-oxine as radiotracer. The standard parameters of the protocol are highlighted in dark yellow.

Experiment	CODE	Buffer	Cell number *10^6	Cell line	Labelling Activity [MBq]	V-Ratio	LE [%]
SOPIxxx	CCI	Saline	n.r.	n.r	4–37	n.r.	n.r.
SOPI027b	CCIJ	PBS	0.53	PANC-1	0.69	1:1	38
			0.90	AR42J			41
			0.84	CHO K1 PSMA			41
			0.69	CHO K1 GRPR			42

Labelling of platelets

Isolated, non-activated platelets were labelled as well with the commercially available [^{111}In]In-oxine using the labelling protocol described by the producer (Curium-method). In all experiments, to prevent platelet activation, PPP was always added after incubation. In table 33 in the appendix, all the different labelling experiments are shown in a single table.

Table 22: Results and parameters used of platelet labelling experiments performed according to the Curium-method using [^{111}In]In-oxine as radiotracer. The standard parameters of the protocol are highlighted in dark yellow.

Experiment	Code	Buffer	Labelling Activity [MBq]	V-Tracer [µl]	Shaker [rpm]	LE [%]
SOPIxxx	PCI	Saline	4–37	n.r.	/	n.r.
SOPI026 SOPI021	PCIA	Saline	0.04 0.02	1.5 7	/	26 21
SOPI026	PCIB	Saline	0.32 0.74	14 27	/	27 27
SOPI026 SOPI021	PCIC	Saline	1.62 0.25	53 56	/	52 52
SOPI028	PCID	Saline	1.66, 1.71	58	hand	range 35–54 (n = 2)
SOPI022a	PCIE	Saline	0.76–0.84	209	hand	85 ± 1 (n = 3)
SOPI021	PCIF	Saline	1.38	225	/	87
SOPI021	PCIG	Saline	3.66	600	/	72

SOPI021 and 026 each had four labelling variants carried out with different tracer volumes (see table 22). The activities between the two approaches at similar volumes differ, as the experiments of 021 were performed seven days after the radiotracer delivery was received – those of 026 on the same day. In addition, experiments 028 (three days after delivery) and 022a (eight days after delivery) are also shown in table 22. Both experiments, in contrast to the others, were repeatedly shaken manually. As can be seen in table 22 and figure 12, the platelet labelling efficiency also increases as the tracer volume increases, with an upper limit of an approx. 4:1 ratio. Although the **PICD** and **PICE** experiments were repeatedly shaken manually, the LE obtained also follows this pattern.

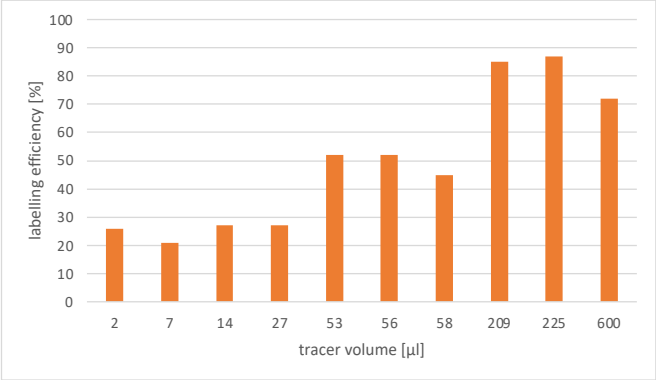

Figure 12: Labelling efficiencies of the platelets labelling experiments with [^{111}In]In-oxine as a function of volume.

Accordingly, in these platelet experiments, the ratio between cell suspension and radiotracer also has a considerable influence on labelling efficiency. Since a similar result was obtained at

a similar volume ratio but at a different activity applied for **PICE** and **PICF**, activity independence can be assumed.

In addition, experiment 028 investigated the influence of tracer dilution. Compared to **PCID** at the same conditions, the lower result of **PCIH** implies that dilution of the tracer reduces PRP uptake (see table 33, appendix).

Two further alterations of the protocol were investigated *via* approach 076 (see table 23). Therefore, the buffer solutions saline (pH = 5.5) was replaced with PBS (pH = 7.0–7.5) and ACD-A (pH = 5.0), respectively, to investigate their effects on the labelling efficiency. In addition, the influence of shaking during incubation was also analysed.

Table 23: Results and parameters used of platelet labelling experiments performed according to the Curium-method using [^{111}In]In-oxine as radiotracer. The standard parameters of the protocol are highlighted in dark yellow.

Experiment	Code	Buffer	Labelling Activity [MBq]	V-Tracer [µl]	Shaker [rpm]	LE [%]
SOPIxxx	PCI	Saline	4–37	n.r.	/	n.r.
SOPI076	PCII	PBS	0.80	200	hand	53
SOPI076	PCIJ	PBS	0.80	200	300	71
SOPI076	PCIK	ACD-A	0.81	200	hand	10
SOPI076	PCIL	ACD-A	0.80	200	300	3

The PBS experiments resulted in 53% and 71% LE, respectively, while the ACD-A experiments yielded much lower efficiencies. For both variations, increased labelling efficiency was obtained in the automatically shaken experiments compared to the manual ones.

4.2.2.2. Labelling Cells using [^{68}Ga]Ga-oxine

<u>Labelling of cells</u>

Overall, 31 cell labelling experiments were performed *via* [^{68}Ga]Ga-oxine without Tris buffer addition. PBS was applied for all cell suspensions. Based on the results of indium-111 oxine, higher cell numbers were used for labelling with gallium-68 oxine. A detailed table is shown in the appendix (see table 34).

Table 24 shows the experiments using [^{68}Ga]Ga-oxine synthesised according to Sinzinger*/1V (pH = 5.5–6.0) as radiotracer. The best result was achieved in the modification **CCGB** at a volume ratio of 3:1 and at high cell numbers.

Table 24: Results and parameters used of PANC-1 labelling experiments performed according to the Curium-method using [^{68}Ga]Ga-oxine as radiotracer, synthesised via Sinzinger/1V. The standard parameters of the protocol are highlighted in dark yellow.*

Experiment	Code	Cell Number *10^6	Labelling Activity [MBq]	V-Ratio	Shaker [rpm]	LE [%]
SOPIxxx	CCG	n.r.	4–37	diff.	/	n.r.
SOPI033b	CCGA	0.57	0.41	10:1	350	7
SOPI058b SOPI059b	CCGB	2.09 3.05	2.5–2.9	3:1	350	11 ± 4 (n = 4)
SOPI033b	CCGC	0.57	1.9	2:1	350	6
SOPI033b	CCGD	0.57	3.9	1:1	350	4

The parameters and results of the labelling experiments carried out with gallium-68 oxine synthesised according to Socan *et al.* after PBS elution (pH = 7.0–7.5) are shown in table 25. In general, the cell number was higher within these approaches. While here, the volume ratios (except for **CIGF**), as well as the activities, were in a similar range, the revolutions per minute of the shaker were varied from 400–750 rpm. The incubation time was 10 min in all experiments.

Table 25: Results and parameters used of PANC-1 labelling experiments performed according to the Curium-method using [^{68}Ga]Ga-oxine as radiotracer, synthesised via Socan et al. The standard parameters of the protocol are highlighted in dark yellow.

Experiment	Code	Cell Number *10^6	Labelling Activity [kBq]	V-Ratio	Shaker [rpm]	LE [%]
SOPIxxx	CCG	n.r.	4–37	n.r.	/	n.r.
SOPI054b SOPI057b	CCGF	1.38–1.67	0.25–0.37	7:1	700	10 ± 1 (n = 4)
SOPI049b	CCGH	1.5–1.7	0.35–0.37	3:1	700	23 ± 0.5 (n = 4)
SOPI053b	CCGI	1.16	0.25	3:1	700	12 ± 0 (n = 2)
SOPI048b	CCGJ	3.16	0.42, 0.44	3:1	750	24 ± 0 (n = 2)
SOPI042b	CCGK	2.72	0.48	3:2	400	9 ± 0 (n = 2)
SOPI043b	CCGL	2.23	0.73, 0.77	3:2	450	8 ± 0 (n = 2)
SOPI044b	CCGM	3.81	0.74, 0.76	3:2	650	19 ± 0 (n = 2)

The two best results were obtained at a volume ratio of 3:1 and at 700–750 rpm with different cell numbers (modification: **CCGH** and **CCGJ**, see table 25). In short, high revolutions per minute as well as a volume ratio of 3:1 seem to favour the labelling efficiency using gallium-68 oxine.

[^{68}Ga]Ga-oxine synthesised according to Man *et al.* (pH = 8.5) was used in higher activities due to better radiochemical yields. Since the synthesis *via* the kit variant resulted in a maximum

volume of 118 µl, the radiotracers were applied in lower quantities (10:1 and 9:1). Comparing the experiments, **CCGL** with a higher cell number and tracer volume resulted in a higher labelling efficiency (see table 26).

Table 26: Results of PANC-1 labelling experiments performed according to the Curium-method using [^{68}Ga]Ga-oxine as radiotracer, synthesised via Man et al. The standard parameters of the protocol are highlighted in dark yellow.

Experiment	Code	Cell Number *10^6	Labelling Activity [MBq]	V-Ratio	T [°C]	Shaker [rpm]	LE [%]
SOPIxxx	CIG	n.r.	4–37	diff.	n.r.	/	n.r.
SOPI063b	CIGN	3.90	3.14, 3.15	10:1	37	700	6 ± 2 (n = 2)
SOPI062b	CIGL	7.24	2.79–2.87	9:1	37	700	11 ± 0.5 (n = 3)

Labelling of platelets

In total, nine labelling approaches of platelets with previously successfully synthesised [^{68}Ga]Ga-oxine were carried out. Table 27 shows the respective approaches with the most important parameters and their resulting cell labelling efficiency (LE); an overview table is shown in the appendix (see table 35).

Table 27: Results of the platelet labelling experiments performed according to the Curium-method using [^{68}Ga]Ga-oxine as radiotracer. The standard parameters of the protocol are highlighted in dark yellow.

Experiment	Code	Buffer	Labelling Activity [MBq]	V-Tracer [µl]	T [°C]	Shaker [rpm]	PPP-Addition [µl]	LE [%]
SOPIxxx	PCG	Saline	4–37	n.r.	r.t.	/	667	n.r.
SOPI022b*	PCGA	Saline	1.3	209	r.t.	/	667	2
SOPI026*	PCGB	Saline	2.3	300	r.t.	/	667	2 ± 0 (n = 2)
SOPI061**	PCGC	PBS	1.3	50	37	300	667	2 ± 0 (n = 2)
SOPI082**	PCGD	PBS	0.16–0.17	25	37	300	/	25 ± 4 (n = 4)

**[^{68}Ga]Ga-oxine synthesised via Sinzinger*/1V. **[^{68}Ga]Ga-oxine synthesised via Man et al.*

First, the Curium-protocol was followed exactly (022b), while in 026 the addition of Tris buffer was omitted. Both radiotracers were synthesised following the protocol of Sinzinger*/1V at a pH of 5.5–6.0. Based on previous results, 209 and 300 µl tracer volumes were chosen for **PCGA** and **PCGB**, respectively. However, the labelling of both experiments only resulted in 2% (n = 3) LE. As described above, cell incorporation cannot be assumed at such low percentages.

In 061 and 083, [^{68}Ga]Ga-oxine was obtained *via* the Man-method at a pH of 8.5 and was added to a platelet suspension in PBS. In both labelling experiments, the suspension was shaken at 300 rpm at 37 °C. **PCGC** resulted also in only 2% LE.

In contrast, the addition of PPP after incubation was omitted in 082, which did not lead to a visible activation of the platelets. Therefore, an average LE of 25% was obtained in the resuspended PRP (see table 27).

Figure 13 compares the different LE of the various labelling variants with gallium-68 oxine. As can be seen, the addition of platelet-poor plasma after incubation has a substantial influence on the labelling efficiency. Without the addition, the uptake in PRP could be clearly increased (**PCGD**, dark blue bar, see figure 13).

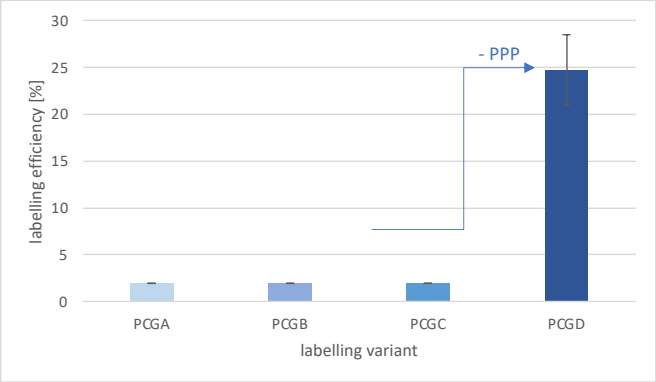

Figure 13: Labelling efficiencies of the platelet labelling experiments using [^{68}Ga]Ga-oxine obtained by different labelling variants, whereby the light blue bars represent the experiments with PPP addition and the dark blue one the one without PPP addition after incubation.

4.2.2.3. Labelling Cells using [^{89}Zr]Zr-oxine

<u>Labelling of cells</u>

All cell labelling experiments using the radiotracer zirconium-89 oxine are summarised in table 36 in the appendix. In total, eighteen cell experiments were performed using [^{89}Zr]Zr-oxine, which was obtained according to Socan *et al*. or Man *et al.* (see table 28). In general, no Tris buffer was added to the radiotracer solution. The cells were resuspended in PBS for all labelling experiments.

Table 28 shows the experiments carried out using [^{89}Zr]Zr-oxine synthesised according to Socan *et al*. after elution with an oxine solution (**CCZA**) or with 50% EtOH/PBS solution (**CCZB**). Both labelling variants were performed at similar conditions. While **CCZA** led to a high mean value of 89 ± 2 (n = 6) LE, 32% labelling efficiency was obtained by **CCZB**. Accordingly, the radiotracer solution (50% EtOH in H_2O) with a pH value of 5 seems to favour the labelling process.

The modifications **CCZC**–**CCZF** were carried out using zirconium-89 oxine synthesised according to Man *et al.* (see table 28). For **CCZC** and **CCZD**, PANC-1 cells were labelled, whereas for **CCZE** and **CCZF**, the cell line AR42J was used. The best result of the zirconium-89 tracers synthesised according to Man *et al.* was achieved at **CCZD** at 650 rpm.

Different incubation conditions ([°C] and rpm) were compared in experiment 079b. For **CIZE,** the cell suspension was incubated at 37 °C at 450 rpm, and for **CIZF** at r.t. using manual, repeated shaking, resulting in a slightly better labelling efficiency for **CIZE** (see table 28).

Table 28: Results and parameters used of PANC-1 labelling experiments performed according to the Curium-method using [^{89}Zr]Zr-oxine as radiotracer, synthesised via Socan et al or Man et al. The standard parameters of the protocol are highlighted in dark yellow.

Experiment	Code	Cell Number *10^6	Labelling Activity [MBq]	V-Ratio	Time [min]	T [°C]	Shaker [rpm]	LE [%]
SOPIxxx	CCZ	n.r.	4–37	n.r.	20	r.t.	/	n.r.
SOPI068b* SOPI067b* SOPI070b*	CCZA	1.56–3.26	0.06–0.10	1000:25	15	37	650	89 ± 2 (n = 6)
SOPI070b**	CCZB	1.61	0.020	1000:25	15	37	650	32
SOPI066c***	CCZC	3.35	0.62, 0.63	1000:30	15	37	650	33 ± 0.5 (n = 2)
SOPI067c*** SOPI070c*** SOPI071b***	CCZD	1.34–1.91	0.36–0.70	1000:25	15	37	650	55 ± 15 (n = 5)
SOPI079b***a	CCZE	2.00	0.38	1000:25	20	37	450	26 ± 4 (n = 2)
SOPI079b***a	CCZF	2.00	0.38	1000:25	20	r.t.	hand	18 ± 0 (n = 2)

**[^{89}Zr]Zr-oxine synthesised via Socan et al. (oxine). **via Socan et al (50%EtOH/PBS). ***via Man et al. [a]Cell line AR42J was used instead of PANC-1.*

Labelling of platelets

The Curium-variant was also applied for the labelling of platelets using zirconium-89 oxine. The radiotracers were mainly obtained *via* Man *et al.* (pH = 8.5), except for the radiotracer of 068 which was obtained *via* Socan *et al.* after an oxine elution (pH = 5.0). Important parameters used are shown in table 29; a complete table is in the appendix (see table 37).

In both, **PCZA** and **PCZB**, a LE of 9% was obtained. In further labelling experiments, the platelets-poor plasma was not added during or after the incubation time, as it was conducted in **PCGD** (see table 27). At 300 rpm, 37 °C and a higher activity, the modification **PCZD** resulted in the best efficiency of 39%. The modifications **PCZE**, with lower activity, and **PCZF**, with saline

as suspension solution, showed a slightly lower LE. Repeated manual shaking, as performed in **PCZC**, resulted in lower LE. However, in all experiments without the addition of PPP, a higher labelling efficiency was achieved than in those with PPP.

Table 29: Results and parameters used of the platelet labelling experiments performed according to the Curium-method using [^{89}Zr]Zr-oxine as radiotracer. The standard parameters of the protocol are highlighted in dark yellow.

Experiment	Code	Buffer	Labelling Activity [MBq]	T [°C]	Shaker [rpm]	PPP-Addition [µl]	LE [%]
SOPIxxx	PCZ	Saline	4–37	r.t.	/	667	n.r.
SOPI068*	PCZA	PBS	0.06	r.t.	300	667	9
SOPI078**	PCZB	PBS	0.48–0.52	r.t	hand	667	9 ± 2 (n = 3)
SOPI080**	PCZC	PBS	0.46–0.47	37	hand	/	30 ± 2 (n = 2)
SOPI080** SOPI081** SOPI083**	PCZD	PBS	0.46–0.53	37	300	/	38 ± 5 (n = 6)
SOPI084**	PCZE	PBS	3.13	37	300	/	39 ± 7 (n = 3)
SOPI081**	PCZF	Saline	0.52	37	300	/	37 ± 5 (n = 2)

**[^{89}Zr]Zr-oxine synthesised via Socan et al. (oxine). **[^{89}Zr]Zr-oxine synthesised via Man et al.*

For a better overview, the labelling efficiencies of the different platelet experiments with zirconium-89 oxine are shown in figure 14. As in the labelling experiments with gallium-68 oxine, the addition of PPP has a considerable influence on the uptake in PRP. The orange bars illustrate the experiments with PPP addition (**PCZA** & **PCZB**), while the yellow bars represent different labelling variants without PPP addition. Figure 14 also shows that gentle shaking during incubation with no platelet activation (**PCZC**, **PCZD** & **PCZE**) influences the labelling efficiency positively. In addition, the uptake of zirconium-89 oxine in PRP seems to be independent of the resuspension buffer, as well as activity-independent (**PCZE** vs. **PCZD/F**).

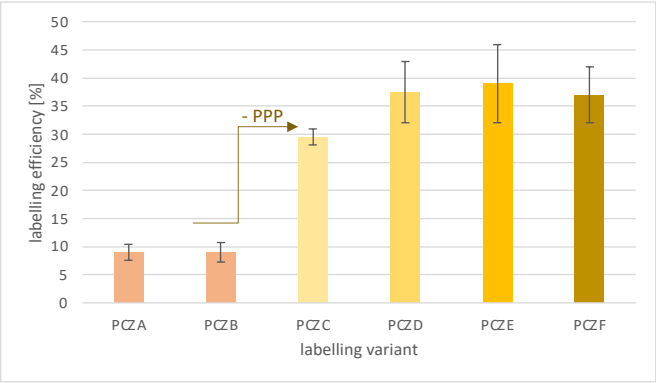

Figure 14: Labelling efficiencies of the platelet labelling experiments using [^{89}Zr]Zr-oxine obtained by different labelling variants, whereby the orange bars represent the experiments with PPP addition and the yellow ones those without PPP addition after incubation.

Figure 15 compares the labelling experiments of platelets with gallium-68 oxine and with zirconium-89 oxine. More specifically, the labelling conditions for **PCGD** were the same as for **PCZD**, except for the activity used. While labelling with [^{68}Ga]Ga-oxine resulted in a mean labelling efficiency of 25 ± 4% (n = 4), [^{89}Zr]Zr-oxine achieved a higher LE of 38 ± 6 (n = 6).

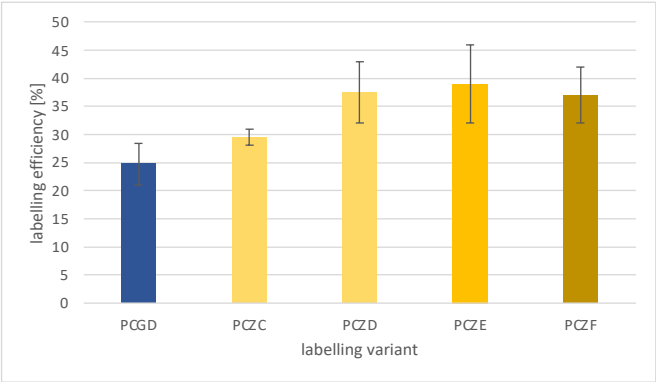

Figure 15: Comparison of the platelet labelling approaches without PPP addition of [^{68}Ga]Ga-oxine (blue) and [^{89}Zr]Zr-oxine (yellow).

5. Discussion

Synthesis: [^{68}Ga]Ga-oxine

[^{68}Ga]Ga-oxine was successfully produced *via* three different syntheses. The various approaches of the synthesis protocols resulted in different yields and radiochemical conversion rates. The Sinzinger-method generally yielded an acceptable mean value of 90% RCC *via* iTLC analysis and 86% RCC after an *n*-octanol extraction. But, the results tended to vary and thus did not provide good reproducibility. In three out of eleven experiments, no complex formation was detected *via* iTLC analysis after 15 min of incubation, but in two of these three experiments, radiochemical transformation was measured after a longer incubation time. In one experiment, however, no complex formation was detected by iTLC measurements even after a longer incubation time. But, in the extraction analysis, a complex formation of 98% was identified. Thus, this result is contrary to the iTLC result as the presence of an organic complex is clearly indicated. Overall, however, the results of the iTLC and extraction analyses yielded quite similar values. The averaged variance between the two analysis methods was about 3%. Thus, the radiochemical conversion of the complex was generally confirmed by two independent analyses.

In addition to the variation in the conversion rates, [^{68}Ga]Ga-oxine complexes according to the protocol of Sinzinger *et al.* showed different stabilities in the crude mixture (8% EtOH in aqueous solution) using the same experimental conditions. The results obtained did not indicate a common stability pattern and thus did not allow a general interpretation of the dissociation process of the radiotracer as a function of time. The literature on the stability of the tracer is also less consistent. Whereas Yano *et al.* reported a shelf life of the gallium(III) complex in the crude matrix (17% EtOH in aqueous solution) of only 30 min[63], Thompson *et al.* described a complex stability of at least 2 h after purification and formulation of the crude complex.[91] Some tracers synthesised according to Sinzinger *et al.* showed a time-limited stability of 30 min as reported by Yano *et al.*[63], leading to the dissociation of 8-hydroxyquinolines and the leaching of gallium-68. In contrast, some of the complexes produced according to Sinzinger *et al.* showed a long shelf life of at least 120 min or 150 min.

To obtain higher reproducible and conversion rates, as well as consistent stability patterns, the influence of the synthesis parameters, incubation time, activity applied as well as the pH value by changing the volume or molarity of the base, on the RCC was investigated:

Prolonged reaction times: Since complex formation of 15 min was observed in two experiments to be insufficient, the time was increased up to 60 min. However, especially for radiotracers with short half-lives, such as gallium-68 ($t_{1/2}$ = 68 min), the synthesis time is limited.[54] In addition to the duration of the synthesis, the time required for the quality tests as well as for the subsequent labelling experiments of the isolated platelets must also be considered. The steps must be kept as short as possible to ensure sufficient activity in the medium. Burke *et al.* even recommended a synthesis time for gallium-68 tracers of less than 10 min to increase the life of the generator and the number of patients per synthesis.[54] Compared to other synthesis protocols, the incubation time of 15 min chosen by Sinzinger *et al.* is relatively long – various other methods used 10 min for the complexation time.[39, 40, 91, 94] Ungersboeck *et al.* chose only 5 min for the complexation based on their result that extending the incubation time up to 90 min does not change the conversion rate.[89]

Applied activities: Furthermore, the activity of the precursor applied was investigated as another possible factor that could affect the conversion rate under the given conditions. However, the activity applied within the activity range of 8–20 MBq showed no substantial influence on the results. The activities used in the unsuccessful syntheses were within the same activity range as those applied in successful complexations with an RCC of > 99%. Accordingly, at least within this activity range, no distinct correlation between the activity of the radio precursor and the resulting complexation rate was determined. The results of a previously published diploma thesis, which focused on improving the synthesis protocol of Sinzinger *et al.*, gave a similar pattern of independence between applied activity and radiochemical conversion of [^{68}Ga]Ga-oxine in an activity range of 2–11 MBq.[90]

Ungersboeck *et al.* reported a significant influence of the amount of ligand as well as by the pH on the synthesis results.[89]

Therefore, in this work, the primary focus was on the regulation of the pH of the reaction solution. pH regulation: To avoid adding an external factor to the reaction solution, such as the pH adjustment performed by Ungersboeck *et al.* using a 10 M NaOH solution[89], the pH was regulated by changing the volume or molarity of sodium acetate solution.

Hence, the concentration of the sodium acetate solution was reduced (Variation M), leading to lower pH values. Some synthesis protocols work with lower salt concentrations at different volume ratios such as La Fuente *et al.* who used a 1 M (2.5 vol.eq.)[94], Thompson *et al.* who applied a 2 M (1 vol.eq.)[91] and Socan *et al.* who worked with a 155 mg/ml sodium acetate

solution (0.2 vol.eq.)[40]. Accordingly, the concentration was reduced to a 1 M and to a 2 M NaOAc solution (0.05 vol.eq.). To avoid altering too many parameters, the volume equivalents of the Sinzinger-method (1 vol.eq. $GaCl_3$, 0.05 vol.eq. sat. NaOAc, and 0.15 vol.eq. oxine) were maintained leading inevitably to a distinct decrease in the pH value resulting in 0–1.0 (1M-method) and in 1.0–1.5 (2M-method). Due to the very low pH, both approaches resulted in significantly poorer yields compared to the original protocol. Gallium(III) is mostly present as Ga^{3+} or $[Ga(H_2O)_6]^{3+}$ in an aqueous solution at pH < 3 and is, therefore, more accessible to possible complexation.[54] But, at these low pH values, the ligand 8-hydroxyquinoline with a pK_a value of 9.89 is mostly found protonated and thus cannot be coordinated.[54, 95] The amount of the protonated oxine form increases as the pH decreases, reflecting the results obtained. Hence, the yields of the 1M-method were significantly lower than those of the 2M-method.

In the second optimisation method (Variation V), the volume of NaOAc was increased while maintaining the saturated concentration, resulting in a higher pH range and a better radiochemical conversion. The improved synthesis results of both approaches (Sinzinger*/1V and 2V) appear to be primarily due to the increased formation of the desired intermediate complex with acetate as the result of the higher pH and the modified volume equivalents. The salt is used to prevent the formation of gallium hydroxide forms, such as $Ga(OH)_3$, $[Ga(OH)]^{2+}$ and $[Ga(OH)_2]^{+}$, by forming an intermediate complex that is preferred over the hydroxide forms but still has a lower stability constant than [^{68}Ga]Ga-oxine.[54] As a result, the precipitation of the hydroxides, which can occur in a pH range of 3–7, is prevented and thus the availability of the metal ion for subsequent complexation with the desired ligands is ensured.[45] The modified volume ratio between gallium(III) and the acetate solution seems to favour the formation of this intermediate complex. Complex formation depends on the ratio between the central atom and coordination partners as well as on the 'transfer reagent' itself and the pH.[96] Citrate intermediate complexes ($4*10^{-4}$ M), for example, are only preferred up to a pH value of 6, before the insoluble $[Ga(OH)_4]^{-}$ precipitation occurs.[45] However, EDTA intermediate complexes ($1*10^{-8}$ M) remain stable up to a pH of 8 without forming any hydroxides.[96] The results of the 2V-method with a mean RCC of 96% indicate that the acetate intermediate complex is predominantly formed up to a pH of 8.0 and is, thus, available for subsequent complexation with the desired ligands. Moreover, Enyedy *et al.* reported that generally, the cold compound gallium-oxine (KP46) occurs at physiological pH mainly in the form of $[GaL_3]$ even at low concentrations.[70]

As a result, the modified protocol of Sinzinger*/1V with a pH of 5.5–6.0 yielded a conversion rate of 94% (iTLC analyses) and showed lower scattering of the results and thus better reproducibility. Similarly, the stability measurements of the complexes according to Sinzinger*/1V (and also 2V) in the crude matrix showed a consistent pattern over time. Here, all radiochemical conversion values obtained over time were robust and hence, the complexes were stable for at least 120–150 min in the crude mixture (8% EtOH in aqueous solution). Therefore, the stability pattern is comparable to the one of the complexes in the formulation matrix (12% EtOH in saline) reported by Thompson *et al*.[91]

However, in the subsequent cell experiments, the labelling efficiencies could not be improved by [^{68}Ga]Ga-oxine synthesised *via* the modified synthesis. Accordingly, the adapted Sinzinger*/1V was replaced by the synthesis protocols of Socan *et al.* and Man *et al*.

The results of the experiments conducted according to Socan *et al.* remained below the mean value of the radiochemical yield given by Socan. Through further elutions, comparable results could be achieved, but solely with increased volume and lower relative activity as well as deterioration of the RCP. Another deviation from the results reported by Socan was observed in the pH of the product. While the elution of the gallium-68 complexes with PBS resulted in a pH of 7.5, Socan *et al.* reported a decreased pH of 5.9 ± 0.9[40]. To a certain extent, a possible pH reduction of the buffer system is possible by adding of the oxine solution with a pH of 5.0 (V = 0.3 ml), which remained in the column (hold up volume = 0.4 ml) during the incubation. The theoretical reduction of the pH value can be calculated *via* the Henderson-Hasselbach equation (see formula 2/ appendix), resulting in a theoretical pH of 6.9. Hence, the published results ranged between pH 5–7[40], while the performed experiments showing a slightly increased pH of 7.5, which might be a variation occurred from using pH stripes. In summary, the cartridge method by Socan *et al.* for synthesis of [^{68}Ga]Ga-oxine showed poor yields after first product elution. Due to the very low yield values, or respectively increased product volume and therefore low activity concentrations, very high starting activities have to be used for sufficient activity for cell labelling experiments. Moreover, additional elution steps increase the overall synthesis time and with regard to radiation protection, such high activities are not desirable in a not automated synthesis approach.

However, [^{68}Ga]Ga-oxine was successfully synthesised *via* the kit version of Man *et al.* with an RCC of 96%. The synthesis requires only one step and can therefore be carried out in a short time, which is preferable for radiometals with short half-lives such as gallium-68 synthesis.[54]

Due to the pre-prepared formulation, only the radio precursor needs to be added during synthesis. The ready-to-use formulation contains HEPES for pH-buffering (pH = 7.9) and polysorbate 80 to reduce non-specific binding to reaction vessels or needles, which is essential for lipophilic complexes such as [^{68}Ga]Ga-oxine. Man *et al*. recommend cell labelling with a RCC ≥ 85% for subsequent cell labelling.[39] Accordingly, the RCC value obtained (96%) clearly corresponds to the acceptable value.

Overall, the synthesis of [^{68}Ga]Ga-oxine according to Man *et al.* resulted in the highest radiochemical conversion of 96%. Using the Socan-method, only a low yield was obtained, but with a good RCP value of 94% at a comparatively long synthesis time. The RCC values obtained according to the protocol of Sinzinger varied with different stability patterns in the crude matrix. Reproducible values with high mean RCC of 94% were then achieved *via* the Sinzinger*/1V modification. Due to the one-step synthesis and consequently rapid performance at high RCC values, the synthesis of [^{68}Ga]Ga-oxine according to Man *et al.* is preferable to the other synthesis protocols.

[^{89}Zr]Zr-oxine

[^{89}Zr]Zr-oxine was successfully produced *via* two protocols, by Socan *et al.* and by Man *et al.* While a high RCC of 97% was obtained *via* the kit variant, the synthesis *via* the on-cartridge version was considerably more challenging. Socan *et al.* recommend PBS for the elution of [^{89}Zr]Zr-oxine from the cartridge.[40] However, since Zr^{4+}-ions have a high binding affinity for phosphates, phosphate-buffered saline was substituted.[73] The highest results were obtained after elution and respectively second loading with precursor solution. The yield was comparable to the reported values by Socan and might even be improved by a higher elution volume (0.3 ml vs. 2 ml). While [^{89}Zr]Zr-oxine was stable in the crude matrix (50% EtOH in aqueous solution) for at least two days, no complex could be detected in 50% EtOH in PBS after two days, indicating a dissociation of the complex in PBS. However, a 50% ethanolic solution with an excess of the ligand 8-hydroxyquinoline as labelling solution is not suitable for subsequent cell experiments (*vide infra*).

Additionally, zirconium-89 oxine was synthesised using the kit formulation within a short time with 97% RCC. The sodium hydroxide solution present in the kit formulation neutralises [^{89}Zr]Zr-oxalate, so that a neutralisation prior with Na_2CO_3 or $NaHCO_3$ is not necessary. Thus, the synthesis can be done in a single step. Moreover, [^{89}Zr]Zr-oxine was relatively stable in the crude matrix for at least 7 days. The recommended conversion rate for subsequent cell

labelling of ≥ 85% was exceeded in all syntheses. For labelling, the solution can be added immediately to the cells resuspended in PBS or saline.[39]

Labelling

Platelets were isolated using two different centrifugation protocols. Furthermore, in vitro cell lines were used due to an easier access, non-invasive and faster approach, whereby the obtained results can be understood as guidelines for platelet labelling. Due to the small size of platelets, 3.6 x 0.7 µm [2], the given examination possibilities did not allow an exact determination of the cell number. However, depending on the blood donor, an approximate range of 270.000–410.000 platelets/µl, which is within the reference range of platelets of a healthy person (reference range: 150.000–450.000/µl [3]), was measured.

The labelling of the platelets according to the protocol of Sinzinger *et al.* with gallium-68 oxine resulted in such low percentages that either instability of the tracer in the cell labelling solution, or insufficient separation of the PPP-phase or unspecific binding, in terms of adhesion of the lipophilic tracer adhered to plastic vessels, can be assumed. Low labelling efficiencies were also obtained by [^{111}In]In-oxine using this protocol for both platelet and PANC-1 cell labelling. Since the uptake of the radiotracer can also depend on the isolation method, especially for blood cells,[19] the method was replaced by the centrifugation protocol of the producer of [^{111}In]In-oxine (Curium-method) for the following labelling experiments. However, the labelling protocol was further modified to achieve the highest possible labelling efficiency using [^{68}Ga]Ga-oxine and [^{89}Zr]Zr-oxine.

The optimal labelling conditions varied from one radiotracer to another. Hence, general patterns in the labelling of PANC-1 cells were found. Therefore, a sufficiently high cell number is required for successful labelling. The labelling efficiency was not influenced by the activity applied, nor by the different cell lines. However, the volume ratio between cell suspension and tracer had a considerable influence on the LE regardless of the radiotracer used. In general, improved results were obtained with higher volumes of the radiotracers [^{111}In]In-oxine and [^{68}Ga]Ga-oxine up to a threshold ratio of 4:1 or 3:1, respectively. This influence was not examined for zirconium-89 oxine as the volume was standardised to 25 µl based according to Man *et al*. who recommends a cell suspension:radiotracer ratio of 30:1 for labelling WBCs.[39] However, it can be assumed that the LE can be increased by higher volume ratios.

For [^{68}Ga]Ga-oxine and [^{89}Zr]Zr-oxine, automatic shaking of the incubation solution at 37 °C was also found to be favourable in the PANC-1 experiments. For platelets, shaking of the

incubation solution is quite limited due to a possible activation and subsequent clotting of the cells. Moreover, cell incorporation of the lipophilic oxine-radiotracers is supposed to be independent of temperature, time or shaking, as the mechanism in the literature is described as passive transport through the lipophilic cell membrane.[19, 36, 87, 88, 97] However, Roca *et al.* recommend gently shaking the suspension to prevent sedimentation of the cells during incubation.[36] As observed in the platelet labelling with [^{89}Zr]Zr-oxine, gentle swirling did not activate the platelets but increased the uptake in the PRP. The temperature was raised to 37 °C, although Man *et al.* reported temperature independence in cell labelling using zirconium-89 oxine.[88] However, since Sato *et al.* reported a lower LE due to a weaker non-specific interaction between the radiotracer zirconium-89 oxine and different cells at 37 °C, adjusting the temperature accordingly could also decrease the labelling efficiency.[87]

Furthermore, the influence of the buffer system of the cell suspension was investigated, whereby ACD-A solution (pH = 5.0) resulted in a considerable deterioration of LE. The use of PBS (pH = 7.4) and saline (pH = 5.5) resulted in similar LE for [^{111}In]In-oxine and for [^{89}Zr]Zr-oxine. To avoid a phosphate-buffered salt solution for the labelling experiments with zirconium-89-oxine, a HEPES buffer system might serve as an alternative. However, many labelling experiments of diverse cell types resuspended in PBS using zirconium-89 oxine as radiotracer have been reported.[83, 87, 98]

In addition, to prevent the activation of the platelets, it is recommended to add the previously separated platelet-poor plasma after incubation directly to the cell suspension-tracer mixture before centrifugation.[93] As the results for gallium-68 oxine and for zirconium-89 oxine showed, the labelling efficiency was remarkably increased by omitting this PPP addition. While the uptake of gallium-68 oxine in PRP did not exceed 2% in the labelling experiments with PPP addition, 25% uptake was obtained without adding platelet-poor plasma. A similar increase was observed by zirconium-89 oxine from only 9% to 39% labelling efficiency.

Similar to In^{3+}, Ga^{3+} and Zr^{4+} ions bind to plasma proteins such as transferrin, therefore it is essential to ensure plasma protein-free labelling conditions for platelet labelling using these radiometals.[19, 73, 80] Due to the very similar chemical properties to Fe^{3+}, Ga^{3+} ions form very stable complexes with the iron transport protein transferrin (logK = 20.3).[45, 52, 54] The labelling of platelets with [^{111}In]In-oxine can reach 90% LE after only 5 min.[29] Indium-111 oxine has a lower stability constant compared to gallium-68 oxine, so a faster dissociation of the ligand oxine and corresponding trapping within the cell due to binding to cytoplasmic proteins can

be assumed. Due to the slightly increased binding constant of [^{68}Ga]Ga-oxine, this dissociation process is slower.[63] Enyedy *et al.* even reported stability of the cold complex gallium-oxine (KP46) for several hours under cellular conditions.[70] However, the undissociated complex might possibly diffuse out of the cell, and thus is not trapped inside the cell.[63] Yet, repeated diffusion through the cell membrane is still possible. But, when platelet-poor plasma is added at a certain point of the labelling procedure, dissociation of the complex outside the platelets occurs preferably, leading to a low LE of platelets. Accordingly, Yano *et al.* avoided the addition of previously separated PPP during the labelling process of platelets with gallium-68 oxine.[63] Regarding zirconium-89 oxine, Man *et al.* reported a lower LE for WBC labelling compared to indium-111 oxine under the same conditions due to a possible slower dissociation process within the cell.[39]

Furthermore, the highest labelling efficiency of 89% was achieved *in vitro* (PANC-1 cells) with zirconium-89 oxine, synthesised according to Socan *et al.* after an oxine elution with a pH of 5.0. However, the 50% ethanolic solution contains an excess of 8-hydroxyquinoline. After the diffusion into the cell, the complex dissociates and the chelator oxine is released from the cell and removed from the labelled platelets by subsequent centrifugation.[36, 62, 97]. Although Man *et al.* reported 99.87% unbound oxine (50 µg in the formulation mixture), the *in vivo* properties of the leukocytes did not change. In addition, a free chelator, as well as unbound radiometal, can be removed by means of an additional washing step.[39] In contrast, Burke *et al.* found effects on the chemotaxis of labelled cells by oxine tracers.[32] Additionally, Zakhireh *et al.* recommended the use of the lowest possible concentrations of oxine (< 10 µg/10^7 cells) to ensure cell viability.[99] The different observations seem to vary according to cell types or labelling protocols.[32] Moreover, the viability of the labelled cells in this experiment was not analysed, so an uptake by non-viable cells cannot be ruled out. Therefore, a 50% ethanolic solution with enormous excess of oxine seems hardly suitable for cell labelling. However, the ethanol content in the suspension is < 2%. Also, for the platelets no coagulation was observed during the experiments assuming viability.

Taken together, with the optimised labelling procedure, the isolated platelets were labelled with 25% [^{68}Ga]Ga-oxine. With [^{89}Zr]Zr-oxine, a higher LE of 39% was obtained by the optimised labelling method. Compared to the reported 90% LE of [^{111}In]In-oxine[29], these values are lower. However, given the recommendation by Man *et al.* of a patient dose of 9–

10 MBq for [^{89}Zr]Zr-oxine[39], the initial activity of the radio precursor [^{89}Zr]Zr-oxalate is 24–26 MBq. The recommendation as SOP can be found in the appendix.

6. Conclusion and Outlook

[^{68}Ga]Ga-oxine and [^{89}Zr]Zr-oxine were synthesised by different methods (pot, on-cartridge, kit synthesis) with adaption of various parameters, leading to appropriate results with regard to yield, conversation and radiochemical purity for further studies. The main goal of this thesis was to radiolabel platelets with a PET tracer and compare to labelling efficiencies of [^{111}In]In-oxine, a SPECT tracer established for cell labelling. However, [^{68}Ga]Ga-oxine might not be a suitable candidate for *in vivo* application, showing cell labelling efficiencies of max. 25%. Furthermore, it is unclear if the half-life of gallium-68 is suitable for the *in vivo* kinetics of platelets (biological half-life of 8–10 days). On the contrary, [^{89}Zr]Zr-oxine showed labelling efficiencies in platelets of almost 40%. Moreover, with a half-life of 78 h Zr-89 might be beneficial for platelets imaging studies. The main finding was that PPP addition, as described in literature, hampers the cell labelling efficiency massively. Hence, following the suggested kit radiosynthesis (Man *et al.*) and cell labelling protocol (25 µl tracer, cells in PBS, pH = 7.4, 37 °C, 300 rpm, 20 min) [^{89}Zr]Zr-oxine is a suitable candidate for *in vivo* application.

Studies on the stability of [^{89}Zr]Zr-oxine under physiological conditions will be required. In addition, viability of the labeled platelets can be analysed by Trypan Blue exclusion methods, and cell disruption methods can examine the site of binding of the free radiometal.

7. Reference

[1] Ghoshal, K., & Bhattacharyya, M. (2014). Overview of platelet physiology: Its hemostatic and nonhemostatic role in disease pathogenesis. *The Scientific World Journal*, *2014*, 1–16. https://doi.org/10.1155/2014/781857

[2] Jurk, K., & Kehrel, B. E. (2005). Platelets: Physiology and biochemistry. *Seminars in Thrombosis and Hemostasis*, *31*(4), 381–392. https://doi.org/10.1055/s-2005-916671

[3] Thomas, S. G. (2019). The structure of resting and activated platelets. In A. Michelson, M. Cattaneo, A. L. Frelinger, & P. J. Newman (Eds.), *Platelets* (pp. 47–77). Academic Press. https://doi.org/10.1016/C2016-0-03693-8

[4] Yun, S., Sim, E., Goh, R., Park, J., & Han, J. (2016). Platelet activation: The mechanisms and potential biomarkers. *BioMed Research International*, *2016*, 1–5. https://doi.org/10.1155/2016/9060143

[5] Gentry, P. A. (1992). The mammalian blood platelet: Its role in haemostasis, inflammation and tissue repair. *Journal of Comparative Pathology*, *107*(3), 243–270. https://doi.org/10.1016/0021-9975(92)90002-c

[6] Bledzka, K., Qin, J., & Plow, E. F. (2019). Integrin αIIbβ3. In A. D. Michelson, M. Cattaneo, A. L. Frelinger, & P. J. Newman (Eds.), *Platelets* (pp. 227–241). Academic Press. https://doi.org/10.1016/B978-0-12-813456-6.00012-6

[7] Lohrke, J., Siebeneicher, H., Berger, M., Reinhardt, M., Berndt, M., Mueller, A., Zerna, M., Koglin, N., Oden, F., Bauser, M., Friebe, M., Dinkelborg, L. M., Huetter, J., & Stephens, A. W. (2017). ^{18}F-GP1, a novel PET tracer designed for high-sensitivity, low-background detection of thrombi. *Journal of Nuclear Medicine*, *58*(7), 1094–1099. https://doi.org/10.2967/jnumed.116.188896

[8] Stephens, A. W., Koglin, N., & Dinkelborg, L. M. (2018). Commentary to ^{18}F-GP1, a novel PET tracer designed for high-sensitivity, low-background detection of thrombi: Imaging activated platelets in clots — Are we getting there? *Molecular Imaging*, *17*, 1–4. https://doi.org/10.1177/1536012117749052

[9] Ziegler, M., Alt, K., Paterson, B. M., Kanellakis, P., & Bobik, A. (2016). Highly sensitive detection of minimal cardiac ischemia using positron emission tomography imaging of activated platelets. *Scientific Reports*, *6*(38161), 1–10. https://doi.org/10.1038/srep38161

[10] Kim, C., Lee, J. S., Han, Y., Chae, S. Y., Jin, S., Sung, C., Son, H. J., Oh, S. J., Lee, S. J., Oh, J. S., Cho, Y., Kwon, T., Lee, D. H., Jang, S., Kim, B., Koglin, N., Berndt, M., Stephens, A. W., & Moon, D. H. (2019). Glycoprotein IIb/IIIa receptor imaging with ^{18}F-GP1 PET for acute venous thromboembolism: An open-label, nonrandomized, phase 1 study. *Journal of Nuclear Medicine*, *60*(2), 244–249. https://doi.org/10.2967/jnumed.118.212084

[11] Hugenberg, V., Zerna, M., Berndt, M., Zabel, R., Preuss, R., Rolfsmeier, D., Wegener, J., Fox, H., Kassner, A., Milting, H., Koglin, N., Stephens, A. W., Gummert, J. F., Burchert, W., & Deutsch, M. (2021). GMP-compliant radiosynthesis of [^{18}F]GP1, a novel PET tracer for the detection of thrombi. *Pharmaceuticals*, *14*(739), 1–17. https://doi.org/10.3390/ph14080739

[12] Bing, R., Deutsch, M.-A., Sellers, S. L., Corral, C. A., Andrews, J. P. M., van Beek, E. J. R., Bleiziffer, S., Burchert, W., Clark, T., Dey, D., Friedrichs, K., Gummert, J. F., Koglin, N., Leipsic, J. A., Lindner, O., MacAskill, M. G., Milting, H., Pessotto, R., Preuss, R., … Newby, D. E. (2022). F-GP1 positron emission tomography and bioprosthetic aortic valve thrombus. *JACC: Cardiovascular Imaging*, *15*(6), 1107–1120. https://doi.org/10.1016/j.jcmg.2021.11.015

[13] Gremmel, T., Frelinger, A. L., & Michelson, A. D. (2016). Platelet Physiology. *Seminars in Thrombosis and Hemostasis*, *42*(03), 191–204. https://doi.org/10.1055/s-0035-1564835

[14] Rodrigues, M., & Sinzinger, H. (1994). Platelet labeling - Methodology and clinical applications. *Thrombosis Research*, *76*(5), 399–432. https://doi.org/10.1016/0049-3848(94)00137-3

[15] Seabold, J. E., Conrad, G. R., Kimball, D. A., Ponto, J. A., & Bricker, J. A. (1988). Pitfalls in establishing the diagnosis of deep venous thrombophlebitis by indium-111 platelet scintigraphy. *Journal of Nuclear Medicine*, *29*(7), 1169–1180.

[16] Fenech, A., Hussey, J. K., Smith, F. W., Dendy, P. P., Bennett, B., & Douglas, A. S. (1981). Diagnosis of deep vein thrombosis using autologous indium-Ill-labelled platelets. *British Medical Journal, 282*(6269), 1020–1022. https://doi.org/10.1136/bmj.282.6269.1020

[17] Davis, H. H., Siegel, B. A., Heinrich Joist, J., Heaton, W. A., Mathias, C. J., Sherman, L. A., & Welch, M. J. (1978). Scintigraphic detection of atherosclerotic lesions and venous thrombi in man by indium-111-labelled autologous platelets. *The Lancet*, *311*(8075), 1185–1187. https://doi.org/10.1016/s0140-6736(78)90972-8

[18] Ezekowitz, M. D., Leonard, J. C., Smith, E. O., Allen, E. W., & Taylor, F. B. (1981). Identification of left ventricular thrombi in man using indium-111-labeled autologous platelets: A preliminary report. *Circulation*, *63*(4), 803–810. https://doi.org/10.1161/01.cir.63.4.803

[19] Gawne, P. J., Man, F., Blower, P. J., & T. M. de Rosales, R. (2022). Direct cell radiolabeling for *in vivo* cell tracking with PET and SPECT imaging. *Chemical Reviews*, *122*(11), 10266–10318. https://doi.org/10.1021/acs.chemrev.1c00767

[20] Stratton, J. R., Ballem, P. J., Gernsheimer, T., Cerqueira, M., & Slichter, S. J. (1989). Platelet destruction in autoimmune thrombocytopenic purpura: Kinetics and clearance of indium- 111-labeled autologous platelets. *Journal of Nuclear Medicine*, *30*(5), 629–637.

[21] International Atomic Energy Agency. (2015). Clinical Use of Radiolabelled Cells. In *Radiolabelled autologous cells: Methods and standardization for clinical use* (pp. 57–77).

[22] Van der Meer, P. F., Tomson, B., & Brand, A. (2010). In vivo tracking of transfused platelets for recovery and survival studies: An appraisal of labeling methods. *Transfusion and Apheresis Science*, *42*(1), 53–61. https://doi.org/10.1016/j.transci.2009.10.007

[23] Mathias, C. J., & Welch, M. J. (1984). Radiolabeling of platelets. *Seminars in Nuclear Medicine*, *14*(2), 118–127.

[24] Kotzé, H. F., Heyns, A. du P., Lötter, M. G., Pieters, H., Roodt, J. P., Sweetlove, A. M., & Badenhorst, P. N. (1991). Comparison of oxine and tropolone methods for labeling human platelets with indium-111. *Journal of Nuclear Medicine*, *32*(1), 62–66.

[25] Blower, J. E., Cooper, M. S., Imberti, C., Ma, M. T., Marshall, C., Young, J. D., & Blower, P. J. (2019). The radiopharmaceutical chemistry of the radionuclides of gallium and indium. *Radiopharmaceutical Chemistry*, 255–271. https://doi.org/10.1007/978-3-319-98947-1_14

[26] Kushwaha, K., Mitra, A., Chakraborty, A., Keshavkumar, B., Tawate, M., Lad, S., Upadhye, T., Dey M. K., Bhoite, R., Satpati, A. K., & Banerjee, S. (2021). On the production of pharmaceutical grade indium-111-chloride in the medical cyclotron from natural cadmium target and its use in formulation of diagnostic patient dose of ^{111}In-pentetreotide for imaging somatostatin receptor overexpression. *Journal of Radioanalytical and Nuclear Chemistry*, *328*(3), 835–846. https://doi.org/10.1007/s10967-021-07652-9

[27] Jivan, S., & Ruth, T. J. (2020). Production of Radionuclides Used in SPECT. In M. R. Kilbourn & P. J. Scott (Eds.), *Handbook of radiopharmaceuticals: Methodology and applications* (pp. 71–87). Wiley. https://doi.org/10.1002/9781119500575.ch4

[28] McAfee, J. G., & Thakur, M. (1976). Survey of radioactive agents for in vitro labeling of phagocytic leukocytes. II. Particles. *Journal of Nuclear Medicine*, *17*, 488–492.

[29] Wistow, B. W., Grossman, Z. D., McAfee, J. G., Subramanian, G., Henderson, R. W., & Roskopf, M. (1978). Labeling of platelets with oxine complexes of Tc-99m and In-111. In vitro studies and survival in the rabbit. *Journal of Nuclear Medicine*, *19*(5), 483–487.

[30] Beck, B. H., Hyunki, H., Kim, H., Samuel, S., Liu, Z., Shrestha, R., Haines, H., Zinn, K., & Lopez, R. D. (2010). Adoptively transferred ex vivo expanded $\gamma\delta$-T cells mediate in vivo antitumor activity in preclinical mouse models of breast cancer. *Brest Cancer Research and Treatment*, *122*, 135–144. https://doi.org/10.1007/s10549-009-0527-6

[31] Gholamrezanezhad, A., Mirpour, S., Bagheri, M., Mohamadnejad, M., Alimoghaddam, K., Abdolahzadeh, L., Saghari, M., & Malekzadeh, R. (2011). In vivo tracking of 111 In-oxine labeled mesenchymal stem cells following infusion in patients with advanced cirrhosis. *Nuclear Medicine and Biology*, *38*(7), 961–967. https://doi.org/10.1016/j.nucmedbio.2011.03.008

[32] Burke, J. E. T., Roath, S., Ackery, D., & Wyeth, P. (1982). The comparison of 8-hydroxyquinoline, tropolone, and Acetylacetone as mediators in the labelling of polymorphonuclear leucocytes with indium-111: A functional study. *European Journal of Nuclear Medicine*, *7*(2). https://doi.org/10.1007/bf00251647

[33] Dewanjee, M. K., Rao, S. A., & Didisheim, P. (1981). Indium-111 tropolone, a new high-affinity platelet label: Preparation and evaluation of labeling parameters. *Journal of Nuclear Medicine*, *22*, 981–987.

[34] Thakur, M. L., McKenney, S. L., & Park, C. H. (1985). Simplified and efficient labeling of human platelets in plasma using indium-111-2-mecaptopyridine-N-oxide: Preparation and Evaluation. *Journal of Nuclear Medicine*, *26*(5), 510–517.

[35] Southcott, L., & Orvig, C. (2021). Inorganic radiopharmaceutical chemistry of oxine. *Dalton Transactions*, *50*, 16451–16458. https://doi.org/10.1039/d1dt02685b

[36] Roca, M., de Vries, E. F., Jamar, F., Israel, O., & Signore, A. (2010). Guidelines for the labelling of leucocytes with ^{111}In-oxine. *European Journal of Nuclear Medicine and Molecular Imaging*, *37*(4), 835–841. https://doi.org/10.1007/s00259-010-1393-5

[37] Thakur, M., Segal, A. W., Welch, M. J., Hopkins, J., & Peters, T. J. (1977). Indium-111-labeled cellular blood components: Mechanism of labelling and intracellular Location in human neutrophils. *Journal of Nuclear Medicine*, *18*(10), 1022–1024.

[38] Oliveri, V., & Vecchio, G. (2016). 8-Hydroxyquinolines in medicinal chemistry: A structural perspective. *European Journal of Medicinal Chemistry*, *120*, 252–274. https://doi.org/10.1016/j.ejmech.2016.05.007

[39] Man, F., Khan, A. A., Carrascal-Miniño, A., Blower, P. J., & T.M. de Rosales, R. (2020). A kit formulation for the preparation of [^{89}Zr]Zr(oxinate)$_4$ for PET cell tracking: White blood cell labelling and comparison with [^{111}In]In(oxinate)$_3$. *Nuclear Medicine and Biology*, *90-91*, 31–40. https://doi.org/10.1016/j.nucmedbio.2020.09.002

[40] Socan, A., Petrik, M., Kolenc Peitl, P., Krošelj, M., Rangger, C., Novy, Z., Svajger, U., Gmeiner, T., & Decristoforo, C. (2019). On-cartridge preparation and evaluation of ^{68}Ga, ^{89}Zr- and ^{64}Cu-precursors for cell radiolabelling. *Nuclear Medicine and Biology*, *71*, 23–31. https://doi.org/10.1016/j.nucmedbio.2019.04.001

[41] Man, F., Gawne, P. J., & Rosales, R. T. M. De. (2019). Nuclear imaging of liposomal drug delivery system: A critical review of radiolabelling methods and applications in nanomedicine. *Advanced Drug Delivery Reviews*, *143*, 134–160. https://doi.org/10.1016/j.addr.2019.05.012

[42] Witney, T. H., & Blower, P. J. (2021). The chemical tool-kit for molecular imaging with radionuclides in the age of targeted and immune therapy. *Cancer Imaging*, *21*(18), 1–14. https://doi.org/https://doi.org/10.1186/s40644-021-00385-8

[43] Bailey, D. L., Sabanathan, D., Aslani, A., Douglas, H., Walsh, B. J., & Lengkeek, N. A. (2021). RetroSPECT: Gallium-67 as a long-lived imaging agent for theranostics. *Asia Oceania Journal of Nuclear Medicine & Biology*, *9*(1), 1–8. https://doi.org/10.22038/AOJNMB.2020.51714.1355

[44] Lewis, M. R., Reichert, D. E., Laforest, R., Margenau, W. H., Shefer, R. E., Klinkowstein, R. E., Hughey, B. J., & Welch, M. J. (2002). Production and purification of gallium-66 for preparation of tumor-targeting radiopharmaceuticals. *Nuclear Medicine and Biology*, *29*(6), 701–706. https://doi.org/10.1016/s0969-8051(02)00330-x

[45] McInnes, L. E., Rudd, S. E., & Donnelly, P. S. (2017). Copper, gallium and zirconium positron emission tomography imaging agents: The importance of metal ion speciation. *Coordination Chemistry Reviews*, *352*, 499–516. https://doi.org/10.1016/j.ccr.2017.05.011

[46] Green, M. A., & Welch, J. (1989). Gallium radiopharmaceutical chemistry. *Nuclear Medicine and Biology*, *16*(5), 435–448.

[47] Bartholomä, M. D. (2012). Recent developments in the design of bifunctional chelators for metal-based radiopharmaceuticals used in positron emission tomography. *Inorganica Chimica Acta*, *389*, 36–51. https://doi.org/10.1016/j.ica.2012.01.061

[48] Wadas, T. J., Wong, E. H., Weisman, G. R., & Anderson, C. J. (2010). Coordinating radiometals of copper, gallium, indium, yttrium, and zirconium for PET and SPECT imaging of disease. *Chemical Reviews*, *110*(5), 2858–2902. https://doi.org/10.1021/cr900325h

[49] Jackson, G. E., & Byrne, M. J. (1996). Metal ion speciation in blood plasma: Gallium-67-citrate and MRI contrast agents. *Journal of Nuclear Medicine*, *37*(2), 379–386.

[50] Bandoli, G., Dolmella, A., Tisato, F., Porchia, M., & Refosco, F. (2009). Mononuclear six-coordinated Ga(III) complexes: A comprehensive survey. *Coordination Chemistry Reviews*, *253*, 56–77. https://doi.org/10.1016/j.ccr.2007.12.001

[51] Dilworth, J. R., & Pascu, S. I. (2015). The radiopharmaceutical chemistry of gallium(III) and indium(III) for SPECT imaging. In N. Long & W.-T. Wong (Eds.), *The Chemistry of Molecular Imaging* (pp. 165–178). Wiley. https://doi.org/https://doi.org/10.1002/9781118854754.ch7

[52] Fani, M., André, João, P., & Maecke, H. R. (2008). Ga-PET: a powerful generator-based alternative to cyclotron-based PET radiopharmaceuticals. *Contrast Media & Molecular Imaging*, *3*, 53–63. https://doi.org/10.1002/cmmi.232

[53] Hacht, B. (2008). Gallium(III) ion hydrolysis under physiological conditions. *Bulletin of the Korean Chemical Society*, *29*(2), 372–376. https://doi.org/10.5012/bkcs.2008.29.2.372

[54] Burke, B. P., & Archibald, S. J. (2020). Labeling with gallium-68. In M. R. Kilbourn & P. J. Scott (Eds.), *Handbook of radiopharmaceuticals: Methodology and applications* (pp. 291–323). Wiley. https://doi.org/10.1002/9781119500575.ch9

[55] Petrik, M., Vlckova, A., Novy, Z., Urbanek, L., Haas, H., & Decristoforo, C. (2015). Selected ^{68}Ga-siderophores versus ^{68}Ga-colloid and ^{68}Ga-citrate: Biodistribution and small animal imaging in mice. *Biomedical papers of the Medical Faculty of the University Palacky, Olomouc, Czechoslovakia*, *159*(1), 60–66. https://doi.org/10.5507/bp.2014.052

[56] Wang, X., Wang, Y., Wu, Q., Liu, J., Liu, Y., Pan, D., Qi, W., Wang, L., Yan, J., Xu, Y., Wang, G., Miao, L., Yu, L., & Yang, M. (2020). Feasibility study of ^{68}Ga-labeled CAR T cells for in vivo tracking using micro-positron emission tomography imaging. *Acta Pharmacologica Sinica*, *42*(5), 824–831. https://doi.org/10.1038/s41401-020-00511-5

[57] Kilbourn, M. R., Rodnick, M. E., & Clark, M. (2020). Production of short half-life PET radionuclides. In M. R. Kilbourn & P. J. Scott (Eds.), *Handbook of radiopharmaceuticals: Methodology and applications* (pp. 45–69). Wiley. https://doi.org/10.1002/9781119500575.ch3

[58] Decristoforo, C. (2012). Gallium-68 – a new opportunity for PET available from a long shelf-life generator – automation and applications. *Current Radiopharmaceuticals*, *5*(3), 212–220. https://doi.org/10.2174/1874471011205030212

[59] Velikyan, I. (2015). [68]Ga-based radiopharmaceuticals: Production and application relationship. *Molecules*, *20*, 12913–12943. https://doi.org/10.3390/molecules200712913

[60] Velikyan, I. (2014). Prospective of [68]Ga-radiopharmaceutical development. *Theranostics*, *4*(1), 47–80. https://doi.org/10.7150/thno.7447

[61] Martiniova, L., Palatis, L. De, Etchebehere, E., & Ravizzini, G. (2016). Gallium-68 in medical imaging. *Current Radiopharmaceuticals*, *9*, 187–207. https://doi.org/10.2174/1874471009666161028150

[62] Welch, M. J., Thakur, M., Coleman, R. E., Patel, M., Siegel, B. A., & Ter-Pogossian, M. M. (1977). Gallium-68 labeled red cells and platelets new agents for positron tomography. *Journal of Nuclear Medicine*, *18*, 558–562.

[63] Yano, Y., Budinger, T. F., Ebbe, S. N., Mathis, C. A., Singh, M., Brennan, K. M., & Moyer, B. R. (1985). Gallium-68 lipophilic complexes for labeling platelets. *Journal of Nuclear Medicine*, *26*(12), 1429–1437.

[64] Freesmeyer, M., Gröber, S., Greiser, J., Seifert, P., Gühne, F., & Drescher, R. (2021). PET/CT with [[68]Ga]gallium-oxine-labeled heat-denatured red blood cells for detection of dystopic splenic tissue. *European Journal of Nuclear Medicine and Molecular Imaging*, *48*(2), 644–646. https://doi.org/10.1007/s00259-020-04899-4

[65] Drescher, R., Gröber, S., Seifert, P., & Freesmeyer, M. (2021). Differentiation of residual splenic tissue from neuroendocrine tumor metastasis on PET/CT with heat-damaged, Ga-68-oxine-labeled red blood cells. *Japanese Journal of Clinical Oncology*, *51*(1), 160–161. https://doi.org/10.1093/jjco/hyaa066

[66] Werner, A., Freesmeyer, M., & Drescher, R. (2022). High-resolution splenic imaging: [[68]Ga]Ga-oxine red blood cell PET/CT for differentiation of splenosis mimicking malignant lymphoma. *Tomography*, *8*(6), 2915–2918. https://doi.org/10.3390/tomography8060244

[67] Valiahdi, S. M., Heffeter, P., Jakupec, M. A., Marculescu, R., Berger, W., Rappersberger, K., & Keppler, B. K. (2009). The gallium complex KP46 exerts strong activity against primary explanted melanoma cells and induces apoptosis in melanoma cell lines. *Melanoma Research*, *19*(5), 283–293. https://doi.org/10.1097/cmr.0b013e32832b272d

[68] Kubista, B., Schoefl, T., Mayr, L., van Schoonhoven, S., Heffeter, P., Windhager, R., Keppler, B. K., & Berger, W. (2017). Distinct activity of the bone-targeted gallium compound KP46 against osteosarcoma cells - synergism with autophagy inhibition. *Journal of Experimental & Clinical Cancer Research*, *36*(52), 1–13. https://doi.org/10.1186/s13046-017-0527-z

[69] Wilke, N. L., Abodo, L. O., Frias, C., Frias, J., Baas, J., Jakupec, M. A., Keppler, B. K., & Prokop, A. (2022). The gallium complex KP46 sensitizes resistant leukemia cells and overcomes BCL-2-induced multidrug resistance in lymphoma cells via upregulation of Harakiri and downregulation of XIAP in vitro. *Biomedicine & Pharmacotherapy*, *156*(113974), 1–11. https://doi.org/10.1016/j.biopha.2022.113974

[70] Enyedy, É. A., Dömötör, O., Varga, E., Kiss, T., Trondl, R., Hartinger, C. G., & Keppler, B. K. (2012). Comparative solution equilibrium studies of anticancer gallium(III) complexes of 8-hydroxyquinoline and hydroxy(thio)pyrone ligands. *Journal of Inorganic Biochemistry*, *117*, 189–197. https://doi.org/10.1016/j.jinorgbio.2012.08.005

[71] Hummer, A. A., Bartel, C., Arion, V. B., Jakupec, M. A., Meyer-Klaucke, W., Geraki, T., Quinn, P. D., Mijovilovich, A., Keppler, B. K., & Rompel, A. (2012). X-ray absorption spectroscopy of an investigational anticancer gallium(III) drug: interaction with serum proteins, elemental distribution pattern, and coordination of the compound in tissue. *Journal of Medicinal Chemistry*, *55*(11), 5601–5613. https://doi.org/10.1021/jm3005459

[72] Bhattacharyya, S., & Dixit, M. (2011). Metallic radionuclides in the development of diagnostic and therapeutic radiopharmaceuticals. *Dalton Transactions*, *40*(23), 6112–6128. https://doi.org/10.1039/c1dt10379b

[73] Holland, J. P. (2020). The radiochemistry of zirconium. In M. R. Kilbourn & P. J. Scott (Eds.), *Handbook of radiopharmaceuticals: Methodology and applications* (pp. 343–374). Wiley. https://doi.org/https://doi.org/10.1002/9781119500575.ch11

[74] Wiberg, E., Wiberg, N., & Holleman, A. F. (2007). *Lehrbuch der anorganischen Chemie*. W. de Gruyter.

[75] Davydov, Y. P., Davydov, D. Y., & Zemskova, L. M. (2006). Speciation of Zr(IV) radionuclides in solutions. *Radiochemistry*, *48*(4), 358–364. https://doi.org/10.1134/s1066362206040084

[76] Dilworth, J. R., & Pascu, S. I. (2018). The chemistry of PET imaging with zirconium-89. *Chemical Society Reviews*, *47*(8), 2554–2571. https://doi.org/10.1039/c7cs00014f

[77] La, M. T., Tran, V. H., & Kim, H. (2019). Progress of coordination and utilization of zirconium-89 for positron emission tomography (PET) studies. *Nuclear Medicine and Molecular Imaging*, *53*, 115–124. https://doi.org/https://doi.org/10.1007/s13139-019-00584-z

[78] Zhang, Y., Hong, H., & Cai, W. (2011). Pet tracers based on zirconium-89. *Current Radiopharmaceuticals*, *4*(2), 131–139. https://doi.org/10.2174/1874471011104020131

[79] Brandt, M., Cardinale, J., Aulsebrook, M. L., Gasser, G., & Mindt, T. L. (2018). An overview of PET radiochemistry, part 2: Radiometals. *Journal of Nuclear Medicine*, *59*(10), 1500–1506. https://doi.org/10.2967/jnumed.117.190801

[80] Abou, D. S., Ku, T., & Smith-Jones, P. M. (2011). In vivo biodistribution and accumulation of ^{89}Zr in mice. *Nuclear Medicine and Biology*, *38*(5), 675–681. https://doi.org/10.1016/j.nucmedbio.2010.12.011

[81] Jalilian, A. R., & Osso, J. A. (2017). Production, applications and status of zirconium-89 immunoPET agents. *Journal of Radioanalytical and Nuclear Chemistry*, *314*(1), 7–21. https://doi.org/10.1007/s10967-017-5358-z

[82] Charoenphun, P., Meszaros, L. K., Chuamsaamarkkee, K., Sharif-Paghaleh, E., Ballinger, J. R., Ferris, T. J., Went, M. J., Mullen, G. E., & Blower, P. J. (2014). [^{89}Zr]oxinate$_4$ for long-term in vivo cell tracking by positron emission tomography. *European Journal of Nuclear Medicine and Molecular Imaging*, *42*(2), 278–287. https://doi.org/10.1007/s00259-014-2945-x

[83] Khan, A. A., Man, F., Faruqu, F. N., Kim, J., Al-Salemee, F., Carrascal-Miniño, A., Volpe, A., Liam-Or, R., Simpson, P., Fruhwirth, G. O., Al-Jamal, K. T., & T. M. de Rosales, R. (2022). PET imaging of small extracellular vesicles via [^{89}Zr]Zr(oxinate)$_4$ direct radiolabeling. *Bioconjugate Chemistry*, *33*(3), 473–485. https://doi.org/10.1021/acs.bioconjchem.1c00597

[84] Edmonds, S., Volpe, A., Shmeeda, H., Parente-Pereira, A. C., Radia, R., Baguña-Torres, J., Szanda, I., Severin, G. W., Livieratos, L., Blower, P. J., Maher, J., Fruhwirth, G. O., Gabizon, A., & T. M. de Rosales, R. (2016). Exploiting the metal-chelating properties of the drug cargo for in vivo positron emission tomography imaging of liposomal nanomedicines. *ACS Nano*, *10*(11), 10294–10307. https://doi.org/10.1021/acsnano.6b05935

[85] Gawne, P. J., Clarke, F., Turjeman, K., Cope, A. P., Long, N. J., Barenholz, Y., Terry, S. Y., & de Rosales, R. T. (2020). PET imaging of liposomal glucocorticoids using ^{89}Zr-oxine: Theranostic applications in inflammatory arthritis. *Theranostics*, *10*(9), 3867–3879. https://doi.org/10.7150/thno.40403

[86] Weist, M. R., Starr, R., Aguilar, B., Chea, J., Miles, J. K., Poku, E., Gerdts, E., Yang, X., Priceman, S. J., Forman, S. J., Colcher, D., Brown, C. E., & Shively, J. E. (2018). PET of adoptively transferred chimeric antigen receptor T cells with ^{89}Zr-oxine. *Journal of Nuclear Medicine*, *59*(10), 1531–1537. https://doi.org/10.2967/jnumed.117.206714

[87] Sato, N., Wu, H., Asiedu, K. O., Szajek, L. P., Griffiths, G. L., & Choyke, P. L. (2015). ^{89}Zr-oxine complex PET cell imaging in monitoring cell-based therapies. *Radiology*, *275*(2), 490–500. https://doi.org/10.1148/radiol.15142849

[88] Man, F., Lim, L., Volpe, A., Gabizon, A., Shmeeda, H., Draper, B., Parente-Pereira, A. C., Maher, J., Blower, P. J., Fruhwirth, G. O., & T.M. de Rosales, R. (2019). In vivo pet tracking of ^{89}Zr-labeled Vγ9Vδ2 T cells to mouse xenograft breast tumors activated with liposomal alendronate. *Molecular Therapy*, *27*(1), 219–229. https://doi.org/10.1016/j.ymthe.2018.10.006

[89] Ungersboeck, J., Groessl, M., Mitterhauser, M., Jakupec, M. A., Eidherr, H., Unfried, P., Kletter, K., Dudczak, R., Keppler, B. K., & Wadsak, W. (n.d.). *Radiosynthesis and quality control of ^{68}Ga@KP46 (^{68}Ga-oxine)*.

[90] Plank, C. (2022). *Platelet isolation and labeling with [^{68}Ga]Ga-oxine* [Unpublished master's thesis]. Universität Wien. https://utheses.univie.ac.at/detail/62668/

[91] Thompson, S., Rodnick, M. E., Stauff, J., Arteaga, J., Desmond, T. J., Scott, P. J., & Viglianti, B. L. (2018). Automated synthesis of [^{68}Ga]oxine, improved preparation of ^{68}Ga-labeled erythrocytes for blood-pool imaging, and preclinical evaluation in rodents. *MedChemComm*, *9*(3), 454–459. https://doi.org/10.1039/c7md00607a

[92] Sinzinger, H., Kolbe, H., Strobl-Jäger, E., & Höfer, R. (1984). A simple and safe technique for sterile autologous platelet labelling using "Monovette" vials. *European Journal of Nuclear Medicine*, *9*(7), 320–322. https://doi.org/10.1007/bf00276462

[93] Curium Netherlands. (2021). *Summary of product characteristics for indium (In111) oxinate, radiopharmaceutical precursor*. 1–4.

[94] de la Fuente, A., Kramer, S., Mohr, N., Pektor, S., Klasen, B., Bausbacher, N., Miederer, M., Zentel, R., & Rösch, F. (2019). ^{68}Ga[Ga]- , ^{111}In[In]-oxine: a novel strategy of in situ radiolabeling of HPMA-based micelles. *American Journal of Nuclear Medicine and Molecular Imaging*, *9*(1), 67–83.

[95] Albert, A., & Phillips, J. N. (1956). Ionization constants of heterocyclic substances. Part II. Hydroxy-derivatives of nitrogenous six-membered ring-compounds. *Journal of the Chemical Society (Resumed)*, 1294–1304. https://doi.org/10.1039/jr9560001294

[96] Staff, K., Brown, M. B., Hider, R. C., Kong, X. L., Friden, P., & Jones, S. A. (2010). Recovering Ga(III) from coordination complexes using pyridine 2,6-dicarboxylic acid chelation ion chromatography. *Biomedical Chromatography*, *24*, 1015–1022. https://doi.org/10.1002/bmc.1402

[97] Sato, N., & Choyke, P. L. (2022). Whole-body imaging to assess cell-based immunotherapy: Preclinical studies with an update on clinical translation. *Molecular Imaging and Biology*, *24*(2), 235–248. https://doi.org/10.1007/s11307-021-01669-y

[98] Patrick, P. S., Kolluri, K. K., Zaw Thin, M., Edwards, A., Sage, E. K., Sanderson, T., Weil, B. D., Dickson, J. C., Lythgoe, M. F., Lowdell, M., Janes, S. M., & Kalber, T. L. (2020). Lung delivery of MSCs expressing anti-cancer protein trail visualised with ^{89}Zr-oxine PET-CT. *Stem Cell Research & Therapy*, *11*(256), 1–12. https://doi.org/10.1186/s13287-020-01770-z

[99] Zakhireh, B., Thakur, M. L., Malech, H. L., Cohen, M. S., Gottschalk, A., & Root, R. K. (1979). Indium-111-labeled human polymorphonuclear leukocytes: Viability, random migration, chemotaxis, bactericidal capacity, and ultrastructure. *Journal of Nuclear Medicine*, *20*(7), 741–747.

8. Abbreviations

%	percent
°C	degree centigrade
µg	microgram
µl	microlitre
ACD	acid citrate dextrose
ACD-A	acid citrate dextrose solution A
ADP	adenosine-di-phosphate
approx.	approximately
AR42J	pancreatic cancer cell line
c	concentration [mol/L]
CAR T cells	chimeric antigen receptor T cells
CHO K1	Chinese hamster ovarian cells
d	day(s)
DFO	desferrioxamine
diff.	different
DMEM	Dulbecco's modified eagle's medium
DMSO	dimethyl sulfoxide
DVT	deep vein thrombosis
EDTA	ethylenediaminetetraacetic acid
EtOH	ethanol
FBS	fetal bovine serum
h	hour(s)
g	gauge
g	gravitational force equivalent
GBq	gigabecquerel
GMP	good manufacturing practice
GP	glycoprotein
GRPR	gastrin-releasing peptide receptor
HEPES	4-(2-hydroxyethyl)-1-piperazineethanesulfonic acid
HSAB	hard and soft acid-base theory
*i*TLC	*instant* thin layer chromatography

*i*TLC-SG	*instant* thin layer chromatography silica gel
K	binding constant
kBq	kilobecquerel
KP46	tris(8-quinolinolato)gallium(III)
LE	labelling efficiency
LoE	loading efficiency
M	molarity [mol/L]
MBq	megabecquerel
max.	mamximum
Mg	milligram
ml	millilitre
MeV	megaelectronvolt
min	minute(s)
MPO	2-mercapto-pyridin-N-oxide
n.d.c.	non-decay corrected
n.p.	not performed
n.r.	not reported
oxine	8-hydroxyquinoline
PANC-1	human pancreatic cancer cell line
PBS	phosphate buffered saline
PET	positron emission tomography
PPP	platelet poor plasma
PRP	platelet rich plasma
PSMA	prostate-specific membrane antigen
pH	potential of hydrogen
P/S solution	penicillin-streptomycin solution
r.t.	room temperature
RBC	red blood cells
RCC	radiochemical conversion
RCP	radiochemical purity
R_f	retardation factor
rpm	revolutions per minute

sat.	saturated
SOP	standard operating procedure
SPE	solid-phase extraction
SPECT	single photon emission computed tomography
T	temperature
$t_{1/2}$	half-life
tropolone	2-hydroxycyclohepta-2,4,6-trien-1-one
V	volume
vol.%	volume percent
vol.eq.	volume equivalent
VTE	venous thromboembolism
vWF	van Willebrand factor
WBC	white blood cells

9. Appendix

Cell Culture – Protocol

General procedure and conditions

The cell lines PANC-1, CHO K1 and AR42J were cultured in DMEM supplemented with 10% FBS, 1% L-glutamine solution and 1% P/S solution. Cultures were maintained at 37 °C under humidified atmosphere containing 5% CO_2. For the radio labelling the cell concentration was approx. about 1–7*10^6 cells/mL in PBS.

Cell Splitting

Cell passaging had to be performed regularly. First, the cells were detached from culture flask. Therefore, the culture medium was removed, before cells were washed with PBS. Trypsination was done for 3 min at 37 °C, before it was stopped by adding culture medium. By dead-cell exclusion *via* Trypan Blue the viable cell number was determined, before the suspension was centrifuged (1200 rpm, 4 min, r.t.). Pellets were resuspended with fresh DMEM. Depending on the number of viable cells, different volumes of cell suspension were added to new culture flasks. They were incubated at 37 °C to allow them to attach and grow.

For the experiments the cell pellet obtained was washed with PBS to remove any remaining medium. Again, the supernatant was withdrawn, and the cells were resuspended in 1 ml PBS or 0.9% NaCl. The suspension was subsequently used for radiolabelling experiments with cell concentration of 0.1–7.2*10^6 cells/ml.

Alternatively, a cell scrapper was used for cell harvesting. Therefore, the cells were detached from the flask mechanically, collected and centrifuged at 1200 rpm for 4 min at r.t.. The pellet was washed with PBS, centrifuged again, and resuspended in PBS before being used for experiments.

Cell Freezing

The cells were first detached from the flask as described before. The obtained cell pellet was resuspended in FBS containing 5% DMSO. The suspension was then transferred into cryovials, which were slowly frozen in a cell cooler for 90 min (cooling: -1 °C per minute), before being stored in a -80 °C freezer.

Cell Thawing

The cells were first carefully adjusted to r.t.. Then, the cells were transferred to a cell culture flask containing DMEM, before incubated under a moisture atmosphere at 37 °C. The medium

was discarded the next day due to the 5% DMSO content. The cells were washed with PBS and new medium was added to allow them to grow.

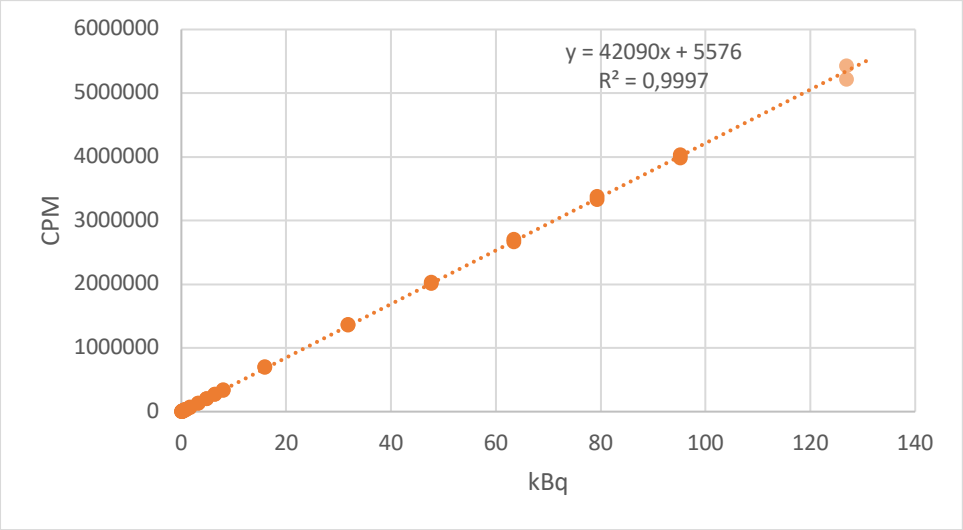

Figure 16: Linearisation measurement of the gamma counter (2480 WIZARD2 3") for the radioisotope [^{68}Ga]Gallium in the activity range of 0–100 kBq.

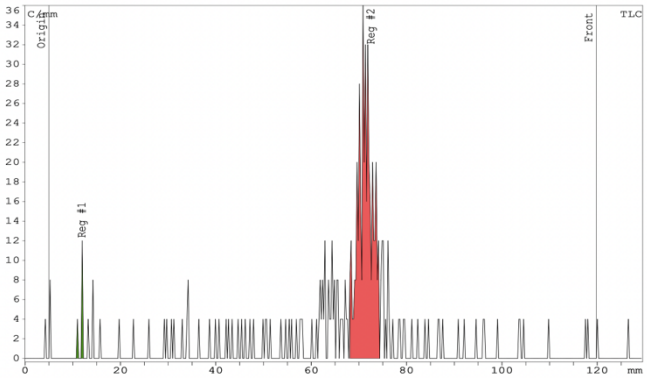

Figure 17: iTLC chromatogram of [^{89}Zr]Zr-oxine with about 96% complex formation (SOPI067b).

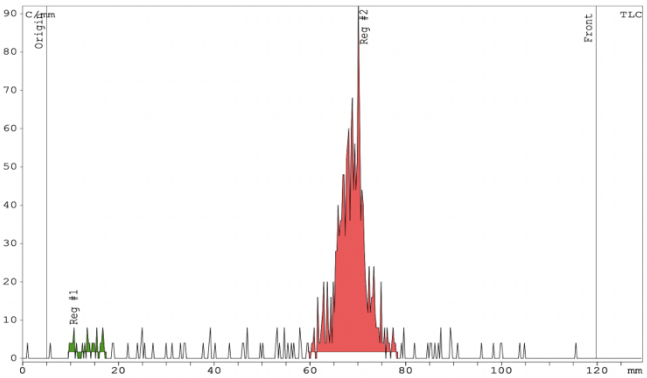

Figure 18: iTLC chromatogram of [^{89}Zr]Zr-oxine with about 98% complex formation (SOPI068b1).

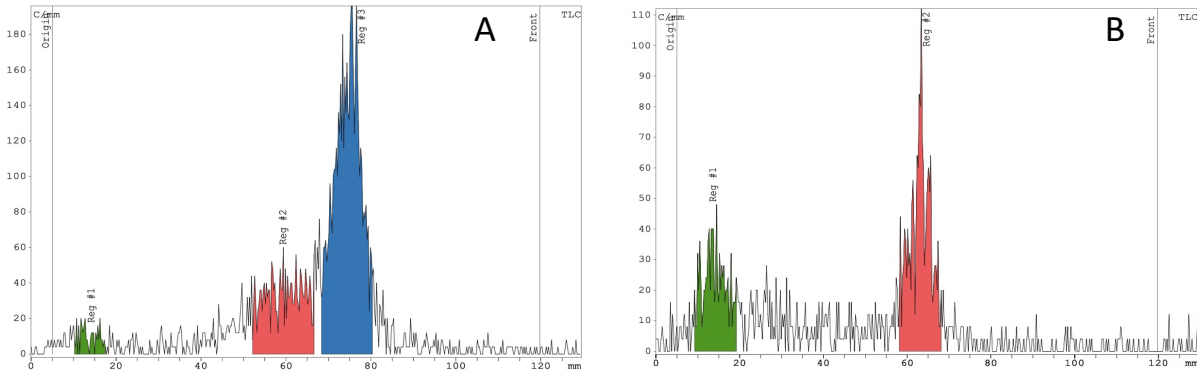

*Figure 19: iTLC chromatograms of [^{89}Zr]Zr-oxine with about 70% complex formation (blue) and a possible side product (red) (**A**; SOPIO70b1) and with about 64% complex formation (**B**, SOPIO70b2).*

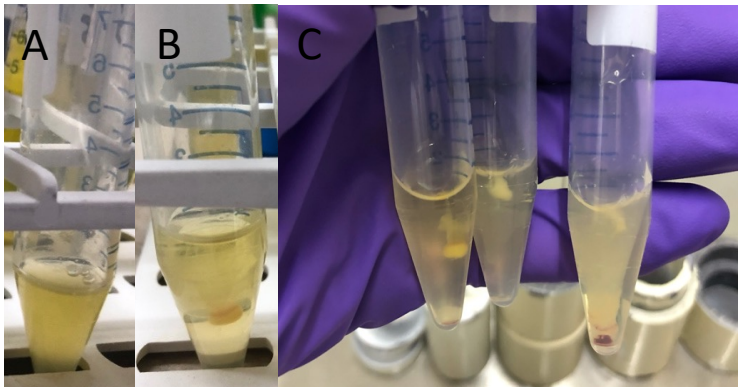

Figure 20: A: Platelet suspension without visible activation. B: Platelet activation in form of a cylindric clot. C: Platelet activation of three different isolated cell samples from different blood samples. In the two samples on the left, a partial, cylindrical clot of platelets is visible. In the right sample, almost the entire platelet suspension (1 ml) has been activated resulting in a more viscous solution also containing a denser clot.

Henderson-Hasselbach equation (2):

$$pH = pK_S - \log\frac{(HA)}{(A^-)} \qquad (2)$$

Tables of the labelling experiments:

Sinzinger-method:

Table 30: Platelet labelling according to the Sinzinger-method using different radiotracers.

Experiment	Code	Tracer	Synthesis-Protocol	Buffer	Labelling Activity [MBq]	V-Ratio	Time [min]	T [°C]	Shaker	LE [%]
SOPIxxx	PS	[^{111}In]In-oxine	n.r.	Tyrode (4°C)	n.r.	n.r.	5	37	/	n.r.
SOPI010	PSGA	[^{68}Ga]Ga-oxine	Sinzinger et al.	Tyrode (4°C)	3.7	1000:360	5	37	/	1
SOPI005	PSGB	[^{68}Ga]Ga-oxine	Sinzinger et al.	Saline + 15% ACD-A	2.3	500:180	5	37	/	1 ± 0 (n = 2)
SOPI020a	PSIA	[^{111}In]In-oxine	/	Tyrode (4°C)	0.05	1000:5	5	37	/	15

Table 31: Cell labelling according to the Sinzinger-method using [^{111}In]In-oxine as radiotracer.

Experiment	Code	Tracer	Buffer	Cell Number*10^6	Labelling Activity [MBq]	V-Ratio	Time [min]	T [°C]	Shaker	LE [%]
SOPIxxx	CS	[^{111}In]In-oxine	Tyrode (4°C)	n.r.	n.r.	n.r.	5	37	/	n.r.
SOPI020c	CSIA	[^{111}In]In-oxine	Saline	0.52	0.05	1000:5	5	37	350	10

Curium-method:

Table 32: Cell labelling according to the Curium-method using [^{111}In]In-oxine as radiotracer.

Experiment	Code	TRIS-Buffer	Buffer	Cell number *10^6	Cell line	Labelling Activity [MBq]	V-Ratio	Time [min]	T [°C]	Shaker [rpm]	LE [%]
SOPIxxx	CCI	+ 0.4 vol.%	Saline	n.r.	n.r.	4–37	n.r.	20	r.t.	/	n.r.
SOPI023b	CCIA	+ 0.4 vol.%	Saline	0.15	PANC-1	0.74–0.75	1000:215	20	r.t.	hand	76 ± 0.5 (n = 3)
SOPI023b	CCIB	+ 0.4 vol.%	Saline	0.15	PANC-1	0.17	20:1	20	r.t.	hand	62
SOPI024b	CCIC	+ 0.4 vol.%	Saline	0.12	PANC-1	0.03,0.04	2:1	20	r.t.	hand	14 ± 0 (n = 2)
SOPI029b	CCID	+ 0.4 vol.%	PBS	0.14–0.19	PANC-1	1.03–1.06	8:1	20	r.t.	hand	61 ± 4 (n = 6)
SOPI029b	CCIE	+ 0.4 vol.%	PBS	0.14–0.19	PANC-1	1.03–1.06	4:1	20	r.t.	hand	71 ± 7 (n = 6)
SOPI029b	CCIF	+ 0.4 vol.%	PBS	0.19	PANC-1	1.01, 1.03	2:1	20	r.t.	hand	82 ± 1 (n = 2)
SOPI030b	CCIG	+ 0.4 vol.%	PBS	0.16	PANC-1	0.52	400:55	20	r.t.	400	61
SOPI030b	CCIH	+ 0.4 vol.%	PBS	0.16	PANC-1	0.89, 0.90	400:35	20	r.t.	400	range 41–58 (n = 2)
SOPI075b	CCII	+ 0.4 vol.%	PBS	1.65	PANC-1	0.25–0.27	1000:25	20	37	650	34 ± 2 (n = 2)
SOPI027b	CCIJ	+ 0.4 vol.%	PBS	0.53	PANC-1	0.69	1:1	20	r.t.	400	38
				0.90*	AR42J						41
				0.84**	CHO K1 PSMA						41
				0.69***	CHO K1 GRPR						42

Table 33: Platelet labelling according to the Curium-method using [^{111}In]In-oxine as radiotracer.

Experiment	Code	TRIS-Buffer	Buffer	Labelling Activity [MBq]	V-Tracer [µl]	Time [min]	T [°C]	Shaker [rpm]	PPP-Addition [µl]	LE [%]
SOPIxxx	PCI	+ 0.4 vol.%	Saline	4–37	n.r.	20	r.t.	/	667	n.r.
SOPI026	PCIA	+ 0.4 vol.%	Saline	0.035	1.5	20	r.t.	/	667	26
SOPI021				0.017	7					21
SOPI026	PCIB	+ 0.4 vol.%	Saline	0.32, 0.74	14	20	r.t.	/	667	27
					27					27
SOPI026	PCIC	+ 0.4 vol.%	Saline	1.62	53	20	r.t.	/	667	52
SOPI021				0.25	56					52
SOPI028	PCID	+ 0.4 vol.%	Saline	1.66, 1.71	58	20	r.t.	hand	667	range 35–54 (n = 2)
SOPI022a	PCIE	+ 0.4 vol.%	Saline	0.76-0.84	209	20	r.t.	hand	667	85 ± 1 (n = 3)
SOPI021	PCIF	+ 0.4 vol.%	Saline	1.38	225	20	r.t.	/	667	87
SOPI021	PCIG	+ 0.4 vol.%	Saline	3.66	600	20	r.t.	/	667	21
SOPI028	PCIH	+ 0.4 vol.%	Saline	1.62, 1.68	58 µl in 942 µl Saline	20	r.t.	hand	667	18 ± 2 (n = 2)
SOPI076	PCII	+ 0.4 vol.%	PBS	0.80	200	20	r.t.	hand	667	53
SOPI076	PCIJ	+ 0.4 vol.%	PBS	0.80	200	20	r.t.	300	667	71
SOPI076	PCIK	+ 0.4 vol.%	ACD-A	0.81	200	20	r.t.	hand	667	10
SOPI076	PCIL	+ 0.4 vol.%	ACD-A	0.80	200	20	r.t.	300	667	3

Table 34: Cell labelling according to the Curium-method using [^{68}Ga]Ga-oxine as radiotracer.

Experiment	Code	Synthesis-Protocol	TRIS-Buffer	Buffer	Cell Number *10^6	Labelling Activity [MBq]	V-Ratio	Time [min]	T [°C]	Shaker [rpm]	LE [%]
SOPIxxx	CCG	/	+ 0.4 vol.%	Saline	n.r.	4–37	n.r.	20	r.t.	/	n.r.
SOPI033b	CCGA	Sinzinger*/1V	/	PBS	0.57	0.41	10:1	20	r.t.	350	7
SOPI058b SOPI059b	CCGB	Sinzinger*/1V	/	PBS	2.09; 3.05	2.5–2.9	3:1	20	r.t.	350	11 ± 4 (n = 4)
SOPI033b	CCGC	Sinzinger*/1V	/	PBS	0.57	1.9	3:1	20	r.t.	350	6
SOPI033b	CCGD	Sinzinger*/1V	/	PBS	0.57	3.9	1:1	20	r.t.	350	4
SOPI033b	CCGE	Sinzinger*/1V	/	PBS	0.57	6.0	1:1.3	20	r.t.	350	4
SOPI054b SOPI057b	CCGF	Socan / PBS	/	PBS	1.38–1.67	0.25–0.37	7:1	10	r.t.	700	10 ± 1 (n = 4
SOPI049b	CCGH	Socan / PBS	/	PBS	1.5–1.7	0.35–0.37	3:1	10	r.t.	700	23 ± 0.5 (n = 4)
SOPI053b	CCGI	Socan / PBS	/	PBS	1.16	0.25	3:1	10	r.t.	700	12 ± 0 (n = 2)
SOPI048b	CCGJ	Socan / PBS	/	PBS	3.16	0.42, 0.44	3:1	10	r.t.	750	24 ± 0 (n = 2)
SOPI042b	CCGK	Socan / PBS	/	PBS	2.72	0.48	3:2	10	r.t.	400	9 ± 0 (n = 2)
SOPI043b	CCGL	Socan / PBS	/	PBS	2.23	0.73, 0.77	3:2	10	r.t.	450	8 ± 0 (n = 2)
SOPI044b	CCGM	Socan / PBS	/	PBS	3.81	0.74, 0,76	3:2	10	r.t.	650	19 ± 0 (n = 2)
SOPI063b	CCGN	Man	/	PBS	3.90	3.14, 3.15	10:1	20	37	700	6 ± 2 (n = 2)
SOPI062b	CCGL	Man	/	PBS	7.24	2.79–2.87	9:1	20	37	700	11 ± 0.5 (n = 3)

Table 35: Platelet labelling according to the Curium-method using [^{68}Ga]Ga-oxine as radiotracer.

Experiment	Code	Synthesis-Protocol	TRIS-Buffer	Buffer	Labelling Activity [MBq]	V-Tracer [µl]	Time [min]	T [°C]	Shaker [rpm]	PPP-Addition [µl]	LE [%]
SOPIxxx	PCG	/	+ 0.4 vol.%	Saline	4–37	n.r.	20	r.t.	/	667	n.r.
SOPI022b	PCGA	Sinzinger*/1V	+ 0.4 vol.%	Saline	1.3	209	20	r.t.	/	667	2
SOPI026	PCGB	Sinzinger*/1V	/	Saline	2.3	300	20	r.t.	/	667	2 ± 0 (n = 2)
SOPI061	PCGC	Man	/	PBS	1.3	50	20	37	300	667	2 ± 0 (n = 2)
SOPI082	PCGD	Man	/	PBS	0.16–0.17	25	20	37	300	/	25 ± 4 (n = 4)

Table 36: Cell labelling according to the Curium-method using [^{89}Zr]Zr-oxine as radiotracer.

Experiment	Code	Synthesis-Protocol	TRIS-Buffer	Buffer	Cell Number*10^6	Labelling Activity [MBq]	V-Ratio	Time [min]	T [°C]	Shaker [rpm]	LE [%]
SOPIxxx	CCZ	/	+ 0.4 vol.%	Saline	n.r.	4–37	n.r.	20	r.t.	/	n.r.
SOPI068b SOPI067b SOPI070b	CCZA	Socan / Oxine	/	PBS	1.56–3.26	0.06–0.10	1000:25	15	37	650	89 ± 2 (n = 6)
SOPI070b	CCZB	Socan / 50% EtOH/PBS	/	PBS	1.61	0.02	1000:25	15	37	650	32
SOPI066c	CCZC	Man	/	PBS	3.35	0.62; 0.63	1000:30	15	37	650	33 ± 0.5 (n = 2)
SOPI067c SOPI070c SOPI071b	CCZD	Man	/	PBS	1.34–1.91	0.36–0.70	1000:25	15	37	650	55 ± 15 (n = 5)
SOPI079b*	CCZE	Man	/	PBS	2.00	0.38	1000:25	20	37	450	26 ± 4 (n = 2)
SOPI079b*	CCZF	Man	/	PBS	2.00	0.38	1000:25	20	r.t.	hand	18 ± 0 (n = 2)

Table 37: Platelet labelling according to the Curium-method using [^{89}Zr]Zr-oxine as radiotracer.

Experiment	Code	Synthesis-Protocol	TRIS-Buffer	Buffer	Labelling Activity [MBq]	V-Tracer [µl]	Time [min]	T [°C]	Shaker [rpm]	PPP-Addition [µl]	LE [%]
SOPIxxx	PCZ	/	+ 0.4 vol.%	Saline	4–37	n.r.	20	r.t.	/	667	n.r.
SOPI068	PCZA	Socan / Oxine	/	PBS	0.06	25	20	r.t.	300	667	9
SOPI078	PCZB	Man	/	PBS	0.48–0.52	25	20	r.t	hand	667	9 ± 2 (n = 3)
SOPI080	PCZC	Man	/	PBS	0.46–0.47	25	20	37	hand	/	30 ± 2 (n = 2)
SOPI080 SOPI081 SOPI083	PCZD	Man	/	PBS	0.46–0.53	25	20	37	300	/	38 ± 5 (n = 6)
SOPI084	PCZE	Man	/	PBS	3.13	25	20	37	300	/	39 ± 7 (n = 3)
SOPI081	PCZF	Man	/	NaCl	0.52	25	20	37	300	/	37 ± 5 (n = 2)

Table 38: List of chemicals used with product number and supplier company.

Product name	Product number	Company
1-Octanol	8.20931	Merck KGaA
4-(2-hydroxyethyl)-1-piperazineethanesulfonic acid (HEPES)	H3375	Sigma Aldrich
8-Hydroxyquinoline	252565	Sigma Aldrich
Anticoagulant Citrate Dextrose Solution	18K01B	Citra Labs LLC
Chloroform	1.02445	Merck KGaA
Dulbecco's Modified Eagle Medium (1X) GlutaMAX™	31966-021	Gibco™
Dulbecco`s Phosphate Buffered Saline (1X)	14190-094	Gibco™
Ethanol	1.00986	Merck KGaA
Ethylacetat	1.00868	Merck KGaA
Fetal Bovin Serum	A4766801	Gibco™
L-Glutamine (200 mM)	25030-024	Gibco™
Hydrochloric Acid (0.1 mol/L)	KT720P	Rotem Industries Ltd
Indium (In-111) oxinate	DRN 4908	Curium Netherlands B.V.
Methanol	34.860	Merck KGaA
Milli Q-water	PR0G000T3	Merck KGaA
Penicilin Streptomycin	15140-122	Gibco™
Phosphate Buffered Saline (1x)	1.123.700.500	MORPHISTO GmbH
Polysorbat 80	8.17061	Merck KGaA
Sodium acetate trihydrate	71188	Sigma Aldrich
Sodium carbonate	451614	Sigma Aldrich
Sodium hydroxide	K1250	Sigma Aldrich
Tris-Buffer	372922	Curium Netherlands B.V.
Trypan Blue Stain (0.4%)	15250-061	Gibco™
Trypsin-EDTA (0.05%, 1X)	25300-054	Gibco™
Tyrode Salt (with bic. Etc vl)	T2397	Sigma Aldrich
Water	95305	Honeywell
Zirconium (Zr-89) oxalate	NEZ308000MC	Perkin Elmer®

Table 39: List of materials used with the product number and supplier company.

Product name	Product number	Company
Centrifree® - Centrifugal Filters	4104	Merck KGaA
Combi-Stopper	4495101	B. Braun Melsungen AG
iTLC-SG-Glass microfiber chromatography paper impregnated with silicagel	SGI0001	Agilent Technologies
Multi-Adapter for S-Monovettes®	141.205	Sarstedt AG & Co.
pH-indicator strips 0.0-6.0	HC033148	Merck KGaA
pH-indicator strips 5.0-10.0	HC900874	Merck KGaA
S-Monovette® 9 ml	21.726.001	Sarstedt AG & Co.
Safety Blood Collection Set (21Gx3/4)	450081	Greiner Bio-One GmbH
Sep-Pak Accell Plus QMA Plus Light Cartridge	WAT023525	Waters™ GmbH
Whatman no.1. paper (ERS shape)	/	Whatman®

Table 40: List of devices used with serial number and company.

Device	Serial number	Company
2480 WIZARD2 3" Automatic Gamma Counter	2480-0010	Perkin Elmer®
AktivimeterISOMED 2010	5.3.6.0.	MED Nuklear-Medizintechnik Dresden GmbH
Galli Ad, 0.74–1.85 GBq, Radionuklidgenerator	1981	IRE ELiT
Gita Star	2009119	Raytest
Luna™ Automatic cell counter	L10001	Logos
miniGita Dual		Elysia Raytest
Rotana 460 RC	5670	Hettich GmbH & Co KG
Universal 320 R	1406	Hettich GmbH & Co KG

SOP: Platelets Labelling with [^{89}Zr]Zr-oxine

Reagents/specific materials:

Reagents/materials	Product number
8-hydroxquinoline (5 mg/10 ml)	252565
HEPES (1 mol/L)	H3375
Polysorbate 80 (10 mg/ml)	8.17061
^{89}Zr-solution ([^{89}Zr]Zr-oxalate in 1M oxalic acid)	NEZ308000MC
Whatman no.1. paper (ERS shape)	/
S-Monovette® 9 ml	21.726.001
Multi-Adapter for S-Monovettes®	141.205
Safety Blood Collection Set (21Gx3/4)	450081

Ultrapure H_2O, 10 M NaOH, EtOAc, ACD-A, Saline/PBS, pH-meter, Whatman® no.1 paper

Preparation of the kit formulation according to Man *et al.*

Precursor solution (V = 10 ml):

Dissolve 5 mg of 8-hydroxyquinoline in approx. 6–7 ml ultrapure H_2O at 80 °C by gently shaking the 10 ml volumetric flask. Let the yellow solution cool down to r.t. before adding 2.38 mg HEPES by shaking until dissolved. In addition, add 1 ml polysorbate 80 (10 mg/ml; Tween® 80) to the solution. Adjust the pH to 7.9–8.0 with aqueous NaOH (10 mol/L). Add ultrapure H_2O to the 10 ml mark and invert the flask to homogenise.

The resulting solution can be kept in the dark for at least six months, it can be autoclaved and/or sterile filtered (use a 0.2 µm PVDF or PES membrane) if required.[39]

Blood samplings *via* Monovettes®:

Cave: The procedure must be carried out as quickly as possible, but also as gently as possible to avoid activation of the platelets.

Add 2 ml of anticoagulant citrate dextrose-A (ACD-A) to the Monovettes® to avoid clotting. For blood withdrawal, use a 21 g butterfly needle, an appropriate adapter and a Monovette®. Slowly draw 7 ml of blood into the Monovette® *via* an unclogged vein. Gently rotate the Monovette® twice and allow them to sediment for about 10 min. Then, centrifuge the samples at 200 g for 15 min at r.t. (brake off). Collect the supernatant (PRP; platelet rich plasma), combine two samples in a Falcon tube and add 15 vol.% ACD-A. Centrifuge the

samples again at 640 g for 15 min at r.t. (brake off) to separate the PPP (platelet poor plasma) from the PRP (cell pellet). After centrifugation, remove the PPP and resuspend the cell pellet gently in an appropriate buffer (V = 1 ml, PBS, saline).[92, 93]

Complexation of the radiotracer

During the second centrifugation:

Add a maximum of 18 µl [^{89}Zr]Zr-oxalate to a 100 µl aliquot of the precursor solution. Swirl it und leave it for 5 min at r.t.[39]

QC of the radiotracer

stationary phase: Whatman no.1 paper

mobile phase: 100% EtOAc

development length: > 6 cm[39]

R_f = 0 → initial educt/colloids

R_f = 1 → product ([^{89}Zr]Zr-oxine)

Labelling of the platelets

Add the radiotracer in the desired volume to the resuspended platelets, swirl it gently at a maximum of 300 rpm at r.t. / 37°C for 20 min. Then, measure the activity. To remove the free, unbound tracer centrifuge the suspension at 1000 g for 15 min at r.t. (brake off). Separate the phases, resuspend the cell pellet and measure the activities of both phases.[92, 93] Determine the labelling efficiency (LE) as follow:[36]

$$LE\ [\%] = \frac{activity\ of\ cell\ fraction\ [MBq]}{activity\ of\ cell\ fraction\ [MBq]\ +\ activity\ of\ supernants\ [MBq]}$$

References of the SOP:

Man, F., Khan, A. A., Carrascal-Miniño, A., Blower, P. J., & T.M. de Rosales, R. (2020). A kit formulation for the preparation of [^{89}Zr]Zr(oxinate)$_4$ for PET cell tracking: White blood cell labelling and comparison with [^{111}In]In(oxinate)$_3$. *Nuclear Medicine and Biology*, *90-91*, 31–40. https://doi.org/10.1016/j.nucmedbio.2020.09.002

Curium Netherlands. (2021). *Summary of product characteristics for indium (In111) oxinate, radiopharmaceutical precursor*. 1–4.

Sinzinger, H., Kolbe, H., Strobl-Jäger, E., & Höfer, R. (1984). A simple and safe technique for sterile autologous platelet labelling using "Monovette" vials. *European Journal of Nuclear Medicine*, *9*(7), 320–322. https://doi.org/10.1007/bf00276462

Roca, M., de Vries, E. F., Jamar, F., Israel, O., & Signore, A. (2010). Guidelines for the labelling of leucocytes with ^{111}In-oxine. *European Journal of Nuclear Medicine and Molecular Imaging*, *37*(4), 835–841. https://doi.org/10.1007/s00259-010-1393-5